In a previous work, Tao et al.[20] divided BAC into three different types (secretory, nonsecretory, and poorly differentiated forms). The secretory type had round-to-oval nuclei with prominent nucleoli. The cytoplasm in the secretory type showed a greater abundance of foamy vacuolated cells than the nonsecretory type. In addition, the secretory type showed tightly packed cell clusters. It is thought that the cellular features of the secretory type resemble the cellular features of GCA at several points.

The limitation of this study is that our study cohort consisted of only imprint smears from the surgically resected tumor. So, some of the aforementioned cytological features may not reflect the true cytological materials (fine-needle aspiration and/or transbronchial brush/washing). The major importance of this work in the future would be to use these cytological features on true cytological materials with the same results obtained in the imprint specimens.

In summary, the cytological features of SRCC are the presence of single tumor cells and nuclear pleomorphism. The cytological features of GCA are the presence of a mucinous background and significant inflammation, and the formation of honeycomb-like cluster. These findings indicate that SRCC could be differentiated from GCA by the cytological material.

References

1. Yamashina M. A variant of early gastric carcinoma: Histologic and histochemical studies of early signet ring cell carcinomas discovered beneath preserved surface epithelium. Cancer 1986;58:1333–1339.
2. Tung SY, Wu CS, Chen PC. Primary signet ring cell carcinoma of colorectum: An age- and sex-matched controlled study. Am J Gastroenterol 1996;91:2195–2199.
3. Kitamura H, Sumikawa T, Fukuoka H, Kanisawa M. Primary signet-ring cell carcinoma of the urinary bladder. Report of two cases with histochemical studies. Acta Pathol Jpn 1985;35:675–686.
4. Randolph TL, Amin MB, Ro JY, Ayala AG. Histologic variants of adenocarcinoma and other carcinomas of prostate: Pathologic criteria and clinical significance. Mod Pathol 1997;10:612–629.
5. Frost AR, Terahata S, Yeh IT, Siegel RS, Overmoyer B, Silverberg SG. The significance of signet ring cells in infiltrating lobular carcinoma of the breast. Arch Pathol Lab Med 1995;119:64–68.
6. Tsuta K, Ishii G, Yoh K, et al. Primary lung carcinoma with signet-ring cell carcinoma components: Clinicopathological analysis of 39 cases. Am J Surg Pathol 2004;28:868–874.
7. Colby TV, Noguchi M, Henschke C, et al. Adenocarcinoma. In: Travis WD, Brambilla E, Muller-Hermelink HK, Harris CC, editors. Pathology and genetics: Tumors of the lung, pleura, thymus and heart. Lyon, France: IARC; 2004. p 35–44.
8. Gemma A, Noguchi M, Hirohashi S, et al. Clinicopathologic and immunohistochemical characteristics of goblet cell type adenocarcinoma of the lung. Acta Pathol Jpn 1991;41:737–743.
9. Tsuta K, Ishii G, Nitadori J, et al. Comparison of the immunophenotypes of signet-ring cell carcinoma, solid adenocarcinoma with mucin production, and mucinous bronchioloalveolar carcinoma of the lung characterized by the presence of cytoplasmic mucin. J Pathol 2006;209:78–87.
10. Hayashi H, Kitamura H, Nakatani Y, et al. Primary signet-ring cell carcinoma of the lung: Histochemical and immunohistochemical characterization. Hum Pathol 1999;30:378–383.
11. Kish JK, Ro JY, Ayala AG, et al. Primary mucinous adenocarcinoma of the lung with signet-ring cells: A histochemical comparison with signet-ring cell carcinomas of other sites. Hum Pathol 1989;20:1097–1102.
12. Maezawa N, Tsuta K, Shibuki Y, et al. Cytopathologic factors can predict invasion in small-sized peripheral lung adenocarcinoma with a bronchioloalveolar carcinoma component. Cancer 2006;108:488–493.
13. Morishita Y, Fukasawa M, Takeuchi M, et al. Small-sized adenocarcinoma of the lung: Cytologic characteristics and clinical behavior. Cancer 2001;93:124–131.
14. Moon KC, Cho SY, Lee HS, et al. Distinct expression patterns of E-cadherin and beta-catenin in signet ring cell carcinoma components of primary pulmonary adenocarcinoma. Arch Pathol Lab Med 2006;130:1320–1325.
15. Nollet F, Berx G, Van Roy F. The role of the E-cadherin/catenin adhesion complex in the development and progression of cancer. Mol Cell Biol Res Commun 1999;2:77–85.
16. Ilyas M, Tomlinson IP. The interactions of APC, E-cadherin and beta-catenin in tumour development and progression. J Pathol 1997; 82:128–137.
17. Shimosato Y, Sobin LH, Spencer H, et al. Histological typing of lung tumours.2nd ed. Geneva, Switzerland: World Health Organization; 1981.
18. Roger V, Nasiell M, Linden M, et al. Cytologic differential diagnosis of bronchiolo-alveolar carcinoma and bronchogenic adenocarcinoma. Acta Cytol 1976;20:303–307.
19. Silverman JF, Finley JL, Park HK, et al. Fine needle aspiration cytology of bronchioloalveolar-cell carcinoma of the lung. Acta Cytol 1985;29:887–894.
20. Tao LC, Weisbrod GL, Pearson FG, et al. Cytologic diagnosis of bronchioloalveolar carcinoma by fine-needle aspiration biopsy. Cancer 1986;57:1565–1570.
21. Loizowski W, Hajdu SI. Cytology and immunocytochemistry of bronchioloalveolar carcinoma. Acta Cytol 1987;31:717–725.
22. Auger M, Katz RL, Johnston DA. Differentiating cytological features of bronchioloalveolar carcinoma from adenocarcinoma of the lung in fine-needle aspirations: A statistical analysis of 27 cases. Diagn Cytopathol 1997;16:253–257.
23. Zaman SS, van Hoeven KH, Slott S, et al. Distinction between bronchioloalveolar carcinoma and hyperplastic pulmonary proliferations: A cytologic and morphometric analysis. Diagn Cytopathol 1997;16:396–401.
24. MacDonald LL, Yazdi HM. Fine-needle aspiration biopsy of bronchioloalveolar carcinoma. Cancer 2001;93:29–34.
25. Ohori NP, Sama Maria EL. Cytopathologic diagnosis of bronchioloalveolar carcinoma: Does it correlate with the 1999 World Health Organization definition? Am J Clin Pathol 2004;122: 44–50.
26. Travis WD, Colby TV, Corrin B, et al. World Health Organization. International histological classification of tumors: Histological typing of lung and pleural tumors. Heidelberg: Springer; 1999.

Whole Genome Comparison of Allelic Imbalance between Noninvasive and Invasive Small-Sized Lung Adenocarcinomas

Hirofumi Nakanishi,[1,4] Shingo Matsumoto,[1,4] Reika Iwakawa,[1] Takashi Kohno,[1] Kenji Suzuki,[2] Koji Tsuta,[3] Yoshihiro Matsuno,[3] Masayuki Noguchi,[5] Eiji Shimizu,[4] and Jun Yokota[1]

[1]Biology Division, National Cancer Center Research Institute; [2]Thoracic Surgery Division and [3]Clinical Laboratory Division, National Cancer Center Hospital, Tokyo, Japan; [4]Division of Medical Oncology and Molecular Respirology, Faculty of Medicine, Tottori University, Tottori, Japan; and [5]Department of Pathology, Institute of Basic Medical Sciences, Graduate School of Comprehensive Human Sciences, Tsukuba University, Ibaraki, Japan

Abstract

Seventy-two small-sized (≤2 cm in diameter) lung adenocarcinomas consisting of 15 noninvasive and 57 invasive tumors were subjected to whole genome allelic imbalance (AI) scanning and mutational analysis of the *EGFR*, *KRAS*, and *TP53* genes to elucidate genetic pathways of early-stage lung adenocarcinomas. The chromosome 13q13 region showed the most frequent AI (58%) and was affected at similar frequencies between noninvasive and invasive tumors (53% and 60%, respectively), as *EGFR* and *KRAS* mutations were. The number of AI regions as well as the frequency of *TP53* mutations in invasive tumors was significantly higher than those in noninvasive ones [9.8 ± 5.6 versus 4.8 ± 2.8 ($P = 0.00002$) and 61% versus 13% ($P = 0.001$), respectively]. In particular, AIs at the chromosome 11p11-p12, 17p12-p13, and 18p11 regions in invasive tumors were significantly more frequent than those in noninvasive ones ($P < 0.01$). The results indicated that noninvasive tumors were developed by *EGFR*, *KRAS*, and 13q alterations and progressed to invasive ones by subsequent alterations of several tumor suppressor genes, including those on 11p11-p12, 17p12-p13, and 18p11 and *TP53*. AI at 8p21 was significantly more frequent in advanced stages (>IA) and associated with worse prognoses ($P = 0.04$) and, thus, would be involved in invasion and/or metastasis of adenocarcinoma cells and useful for the prediction of prognosis of patients with small-sized lung adenocarcinoma. [Cancer Res 2009;69(4):1615–23]

Introduction

Adenocarcinoma is the most common histologic type of lung cancer, and its highly invasive and metastatic phenotypes cause poor prognosis of adenocarcinoma patients (1). The *EGFR* and *KRAS* genes are mutually exclusively mutated in lung adenocarcinomas, and inhibition of activities of these mutants led to the inhibition of adenocarcinoma cell growth (2–5). *EGFR* and *KRAS* mutations have been detected both in noninvasive and invasive adenocarcinomas (6–8); therefore, these alterations are considered to be critical for the development of lung adenocarcinomas, irrespective of their invasiveness. Recently, we showed that *p16* homozygous deletions occur at similar frequencies (~25%) in noninvasive and invasive adenocarcinomas, whereas the frequency of *p53* mutations in invasive ones was much higher than that in noninvasive ones (8). However, phenotypic diversities of adenocarcinomas cannot be explained only by accumulation of these genetic alterations. Importantly, lung adenocarcinomas have been shown to carry allelic losses at tens of chromosomal loci (9–14). Therefore, inactivation of several other tumor suppressor genes could also be involved in the development as well as progression of lung adenocarcinoma. Furthermore, the roles of those allelic losses in the development and/or progression of lung adenocarcinoma are largely unknown.

Small-sized (i.e., ≤2 cm in maximum diameter) lung adenocarcinomas are mainly in early stages and classified into six histologic types, A to F (15). Type A (localized bronchioloalveolar carcinoma) and type B (localized bronchioloalveolar carcinoma with foci of alveolar structural collapse) are noninvasive tumors, whereas type C (localized bronchioloalveolar carcinoma with foci of active fibroblastic proliferation), type D (poorly differentiated adenocarcinoma), type E (tubular adenocarcinoma), and type F (papillary adenocarcinoma with compressive and destructive growth) are invasive ones (1). Types A, B, and C show growth with replacement of bronchioloalveolar cells (replacement growth type); therefore, type A is considered to progress sequentially through type B to type C. In contrast, types D, E, and F show expansive and destructive growth (nonreplacement growth type), and their precursory noninvasive tumors are unknown. The detection of small-sized lung adenocarcinomas is increasing due to recent advances in spiral computed tomography scans (16, 17). However, even after complete resection by surgery, 20% of patients will not survive because of recurrence within 5 years (15). This implies that a subset of small-sized adenocarcinomas have already metastasized to other organs. Therefore, molecular analyses of small-sized adenocarcinomas are important not only to understand the mechanism of multistage lung carcinogenesis but also to identify molecular targets for diagnosis and therapy of patients.

Due to a limited fraction (~4%; ref. 18) and a small volume, only a limited number of small-sized adenocarcinomas have been examined for a few genetic alterations, including *EGFR*, *KRAS*, and *TP53* mutations and allelic imbalance (AI) of a few chromosomal loci (6–8, 19). However, a subset of the alterations, including *TP53* mutations, have been detected more frequently in invasive tumors than in noninvasive tumors. Therefore, it is likely that progression from noninvasive to invasive tumors is caused by accumulation of genetic alterations. Thus, a comprehensive analysis of genetic alterations in small-sized lung adenocarcinoma will give us critical information on molecular mechanisms of lung adenocarcinoma progression as well as genes involved in invasion and metastasis of

Note: Supplementary data for this article are available at Cancer Research Online (http://cancerres.aacrjournals.org/).

H. Nakanishi and S. Matsumoto contributed equally to this work.

Requests for reprints: Jun Yokota, Biology Division, National Cancer Center Research Institute, Tsukiji 5-1-1, Chuo-ku, Tokyo 104-0045, Japan. Phone: 81-3-3547-5272; Fax: 81-3-3542-0807; E-mail: jyokota@ncc.go.jp.

doi:10.1158/0008-5472.CAN-08-3218

adenocarcinoma cells. In this study, 72 small-sized adenocarcinomas, consisting of 15 noninvasive and 57 invasive tumors, were microdissected and subjected to whole genome AI scanning and mutational analysis of the *EGFR*, *KRAS*, and *TP53* genes. Based on the results, a genetic model for the development of noninvasive adenocarcinomas and their progression to invasive adenocarcinomas was depicted, and the association of genetic alterations with clinicopathologic factors was investigated.

Materials and Methods

Patients and tissues. In total, 379 patients with small-sized lung adenocarcinoma underwent curative pulmonary resections from 1993 to 2000 at the National Cancer Center Hospital, Tokyo, Japan. None of them received chemotherapy and radiotherapy before or after surgery. Tumors were pathologically diagnosed according to the tumor-node-metastasis classification (20). In 205 cases, surgical specimens fixed with methanol were available and, thus, were applicable for molecular analyses. Adenocarcinomas were classified into six histologic types: 7 type A, 18 type B, 152 type C, 17 type D, 6 type E, and 5 type F, according to the criteria of small-sized lung adenocarcinoma (15). All type A, B, and D cases and 40 of the 152 type C cases were subjected to DNA extraction. For the validation of association between genetic alterations and prognosis, additional 33 type C and 7 type D tumors were chosen from 380 patients who underwent curative pulmonary resections from 2001 to 2004 at the National Cancer Center Hospital and subjected to DNA extraction.

Cancer cells were obtained by laser capture microdissection using the PixCell Laser Capture Microdissection System (Arcturus Engineering) as previously described (6). Noncancerous lung tissues were obtained from the regions >5 cm from tumors with macroscopically normal morphology in the resected lobes of the lung. Genomic DNAs were extracted as described previously (6). Both the cancerous and noncancerous cell DNAs of sufficient amounts for this study were obtained from 72 cases: 6 type A, 9 type B, 40 type C, and 17 type D cases. This study was undertaken under the approval of the Institutional Review Board of National Cancer Center.

Mutation analysis of the *EGFR/KRAS/TP53* genes. The status of *EGFR/KRAS/TP53* mutations in 30 cases was previously reported (6, 8). Forty-two cases were newly analyzed in this study for mutations in exons 18 to 21 of the *EGFR* gene, in exons 1 to 2 of the *KRAS* gene, and in exons 4 to 8 of the *TP53* gene by genomic PCR and direct sequencing as described previously (6).

Detection of AI by SNP array analysis. AI was examined by the GeneChip Human Mapping 10K Array analysis (Affymetrix, Inc.) according to the method optimized for the analysis of a small amount of DNA samples as described previously (21). Genotype calls of tumors and normal lung tissues were obtained in 80.0% to 94.5% (88.3 ± 3.5) and 83.4% to 97.9% (94.5 ± 2.9), respectively, of the 11,037 SNP sites on the array, and 1,799 to 3,101 loci were informative for detection of AI in the tumors. When a SNP locus was called "homozygous" in tumor DNA and "heterozygous" in the corresponding normal tissue DNA, such a locus was judged as AI in the tumor. The fraction of AI for each tumor was calculated as the fraction of loci judged as AI.

Definition of AI region. AI regions were defined as follows by taking the call error into account. The fraction of error calls for each sample, calculated as the fraction of SNP loci for which normal tissue DNA was called as "homozygous" and tumor DNA as "heterozygous", were 0.0% to 8.9% (1.8 ± 2.3). The appearance of six consecutive "AI" loci by the call error was far less than 1, even for the case with the largest informative loci and the highest probability of call error [i.e., 3,101 informative loci × $(0.089)^6$ = 0.0015]. Thus, AI regions were defined by the criterion of containing at least six consecutive AI loci. Under the same criterion and by combination of SNP array data with spectral karyotyping and array-comparative genomic hybridization data, 1 of 13 (7.7%) trisomic chromosomes was judged as AI, and 14 of 215 (6.5%) AI regions were due to amplification/gain of one allele in our recent study (22). Therefore, one of allelic chromosomal segments was likely to be lost in most (>90%) of AI regions defined in this study.

Microsatellite analysis. Microsatellite markers, *D8S1116* and *D8S322*, were chosen based on the map location and allele frequency in the Japanese population.[6] One hundred picograms of DNA were used for PCR with a set of primers labeled with FAM and NED for *D8S1116* and *D8S322*, respectively. PCR products were run through a 3130xl Genetic Analyzer (Applied Biosystems) and analyzed by the GeneMapper software. A reduction >0.5 or an increase >2.0 of an allele in tumor was determined as AI.

Statistical analysis. Fisher's exact test was used to assess the association of two variables. The differences in the values of fraction of AI and in the number of AI regions between two groups were assessed by the unpaired *t* test. Association of genetic alterations with clinicopathologic characteristics was evaluated by logistic regression analysis (variables with $P \leq 0.2$ were selected). Overall survival of patients with and without genetic alterations was compared by Kaplan-Meier curves and the log-rank test. $P < 0.05$ was considered statistically significant. Statistical analysis was done using JMP software (version 5.1.1, SAS Institute, Inc.).

Results

Clinicopathologic characteristics and the status of *EGFR/KRAS/TP53* mutations. Clinicopathologic characteristics of 72 cases with small-sized lung adenocarcinomas are summarized in Table 1. Adenocarcinomas consisted of 15 noninvasive and 57 invasive tumors. These 72 tumors were of 55 replacement growth types (types A, B, and C) and of 17 nonreplacement growth types (type D). All type A, B, and D cases, whose genomic DNAs were available, in our cohort were enrolled for this study. Fourteen of the 15 noninvasive cases showed good prognoses, whereas 12 of the 17 type D cases showed them. To investigate the association of genetic alterations with prognosis, 40 type C cases consisting of all 19 cases with poor prognosis and 21 random cases with good prognosis were selected from the 152 type C cases in our cohort. Accordingly, the postoperative 5-year overall survival rate of 40 type C cases selected (53%) was considerably lower than those of all 152 type C cases (84%), and the population of advanced stages (>IA) in type C cases selected (53%) was higher than that in all type C cases (24%).

EGFR and *KRAS* mutations were detected in a mutually exclusive manner, being consistent with previous studies (5–8, 23, 24). Frequencies of *EGFR* and *KRAS* mutations were not significantly different between noninvasive tumors and invasive tumors (67%/53% and 13%/11%, respectively; $P > 0.05$). In replacement growth types (types A, B, and C), *EGFR* mutations were detected in ≥50% of the cases, whereas *KRAS* mutations were detected with lower frequencies (≤33%). *EGFR* mutations were detected at a lower frequency in nonreplacement growth types (18%) than in replacement growth types (67%), whereas *KRAS* mutations were detected at similar frequencies in both types (18%/9%). The frequency of *TP53* mutations in invasive tumors was significantly higher than that in noninvasive tumors (61%/13%; $P = 0.001$). *TP53* mutations were detected in none of type A (0%) and in a small subset of type B (22%) but in the majority of type C (53%) and type D (82%) tumors.

Frequency of AI on each chromosome arm. All 72 cases were subjected to a whole-genome AI scanning using a Human Mapping 10K Array covering 11,560 SNP sites placed at a mean interval of

[6] http://www002.upp.so-net.ne.jp/kyama-Q/MS.html

Table 1. Clinicopathologic characteristics and genetic alterations in small-sized lung adenocarcinomas

Clinicopathologic characteristics and genetic alterations*	Subset	Total	Subtype					
			Noninvasive tumors			Invasive tumors		
			All (%)	A (%)	B (%)	All (%)	C (%)	D (%)
		$n = 72$	$n = 15$	$n = 6$	$n = 9$	$n = 57$	$n = 40$	$n = 17$
Gender	Male	35 (49)	8 (53)	5 (83)	3 (33)	27 (47)	17 (42)	10 (59)
	Female	37 (51)	7 (47)	1 (17)	6 (67)	30 (53)	23 (58)	7 (41)
Smoking history	Nonsmoker	36 (50)	8 (53)	2 (33)	6 (67)	28 (49)	22 (55)	6 (35)
	Smoker	36 (50)	7 (47)	4 (67)	3 (33)	29 (51)	18 (45)	11 (65)
Pathologic stage	IA	41 (57)	15 (100)	6 (100)	9 (100)	26 (46)	19 (47)	7 (41)
	>IA	31 (43)	0 (0)	0 (0)	0 (0)	31 (54)†	21 (53)†	1 (59)†
Prognosis‡	Alive	47 (65)	14 (93)	6 (100)	8 (89)	33 (58)	21 (53)	12 (71)
	Dead	25 (35)	1 (7)	0 (0)	1 (11)	24 (42)¶	19 (47)¶	5 (29)
EGFR/KRAS§	E(+)/K(−)	40 (56)	10 (67)	3 (50)	7 (78)	30 (53)	27 (68)	3 (18)†,‖
	E(−)/K(+)	8 (11)	2 (13)	2 (33)	0 (0)	6 (11)	3 (8)	3 (18)
	E(−)/K(−)	24 (33)	3 (20)	1 (17)	2 (22)	21 (37)	10 (25)	11 (65)†,‖
TP53	Mutation(+)	37 (51)	2 (13)	0 (0)	2 (22)	35 (61)†	21 (53)†	14 (82)†,‖
	Mutation(−)	35 (49)	13 (87)	6 (100)	7 (78)	22 (39)	19 (47)	3 (18)
Fraction of AI (%)		24.2 ± 15.4	13.8 ± 8.3	11.4 ± 11.5	15.5 ± 5.5	27.0 ± 15.8¶	27.0 ± 15.7¶	26.9 ± 6.3¶
No. of AI regions		8.7 ± 5.5	4.8 ± 2.8	5.0 ± 3.5	4.7 ± 2.5	9.8 ± 5.6¶	9.9 ± 5.3¶	9.6 ± 6.3¶

*Clinicopathologic characteristics and genetic alterations are shown by the number of cases (%), and fraction of AI and the number of AI regions are shown as mean ± SD.

†$P < 0.05$ for the difference against types A + B by Fischer's exact test.

‡Postoperative 5-y overall survival.

§E(+), *EGFR* mutation (+); E(−), *EGFR* mutation (−); K(+), *KRAS* mutation (+); K(−), *KRAS* mutation (−).

‖$P < 0.05$ for the difference against type C by Fischer's exact test.

¶$P < 0.05$ for the difference against types A + B by unpaired t test.

210 kb. Fraction of AI in total cases was 24.2 ± 15.4% and was twice higher in invasive tumors than in noninvasive tumors ($P = 0.00008$; Table 1). The number of AI regions ranged from 0 to 21 (mean ± SD, 8.7 ± 5.5) and was also twice higher in invasive tumors than in noninvasive tumors ($P = 0.00002$).

At least two AI regions were mapped in all chromosome arms except five acrocentric arms; therefore, common regions of AIs among the 72 cases were defined on each chromosome arm. In total, 52 regions on 39 chromosome arms were defined as common, with two or more regions on 1p, 4q, 5p, 7p, 7q, 8p, 10p, 11p, and 16q (Supplementary Table S1). Frequencies of AI ranged from 8% to 58% (mean ± SD, 25.6 ± 11.8; Table 2). Therefore, regions with frequencies of AI more than mean + SD (37.4) were considered as being "hotspots" of AIs and those more than mean + 2SD (49.2) as being "critical regions" of AIs. There were nine hotspots of AIs, and two critical regions of AIs that were mapped to chromosomes 13q13 and 17p12-p13. The frequency of AI at 13q13 was 58% whereas that at 17p12-p13 was 56%.

In noninvasive tumors and invasive tumors, hotspots as well as critical regions of AIs were also defined based on the value of mean ± SD for the frequencies of AIs. In invasive tumors, hotspots and critical regions were further defined separately in types C and D. In noninvasive tumors, there were 11 hotspots distributed on several chromosome arms and was only one critical region at 13q13. In invasive tumors, there were nine hotspots and two critical regions mapped to 13q13 and 17p12-p13. Similarly, there were eight and seven hotspots and two and two critical regions, respectively, in types C and D. As a whole, 16 of either hotspots or critical regions were identified in total of or in each group of small-sized adenocarcinomas.

Common and differential AIs between noninvasive and invasive tumors. We next searched for regions of AI commonly and differentially affected among noninvasive, invasive, type C, and type D tumors (Table 2). Forty of the 52 regions did not show any significant differences in the frequency of AI among the subtypes. In particular, frequencies of AI in the 13q13 region were similar between noninvasive and invasive tumors (53% and 60%, respectively); therefore, 13q13 was commonly and frequently affected both in noninvasive and invasive tumors. The remaining 12 regions showed significant differences in the frequency of AI among the subtypes. For instance, frequencies of AI at 17p12-p13 in all invasive, type C, and type D tumors were significantly higher than that in noninvasive tumors ($P < 0.01$). Other 11 regions were also significantly more frequently affected by AI in invasive, type C, and/or type D tumors than in noninvasive tumors ($P < 0.05$). Particularly, differences in the frequency of AI at 18p11 and 11p11-p12 regions in type C and type D, respectively, against that in noninvasive tumors were highly significant ($P < 0.01$). In addition, two regions, 11p12 and 17q11, were significantly more frequently affected in both types of invasive tumors than in noninvasive tumors ($P < 0.05$). The other seven

regions were significantly more frequently affected in either type C or type D than in noninvasive tumors ($P < 0.05$). There were no regions that were significantly more frequently affected in noninvasive tumors than in invasive tumors or in either type C or type D tumors. In addition, regions whose frequencies of AI were significantly different between type C and type D tumors were not observed either.

Association of AIs with pathologic stage and prognosis. Nine regions on five different chromosomes showed AIs significantly more frequently in stage >IA tumors than in stage IA tumors

Table 2. Frequency of AI on each chromosome arm in small-sized lung adenocarcinomas

Chromosomal regions with AI	No. of cases (%)								
	Total		Subtype						
			Noninvasive		Invasive				
			A + B		All		C		D
	n = 72		n = 15		n = 57		n = 40		n = 17
1p21-p22	13	(18)	3	(20)	10	(18)	8	(20)	2	(12)
1p13-p21	13	(18)	3	(20)	10	(18)	8	(20)	2	(12)
1q21	13	(18)	3	(20)	10	(18)	7	(18)	3	(18)
2p22-p24	11	(15)	2	(13)	9	(16)	6	(15)	3	(18)
2q35-q37	12	(17)	2	(13)	10	(18)	9	(23)	1	(6)
3p14	24	(33)	4	(27)	20	(35)	14	(35)	6	(35)
3q11	23	(32)	4	(27)	19	(33)	13	(33)	6	(35)
4p12-p13	11	(15)	2	(13)	9	(16)	7	(18)	2	(12)
4q13	17	(24)	3	(20)	14	(25)	12	(30)	2	(12)
4q22	17	(24)	3	(20)	14	(25)	11	(28)	3	(18)
5p15	10	(14)	0	(0)	10	(18)	9	(23)	1	(6)
5p12-p13	10	(14)	2	(13)	8	(14)	7	(18)	1	(6)
5q23	23	(32)	3	(20)	20	(35)	16	(40)	4	(24)
6p11	14	(19)	0	(0)	14	(25)*,†	8	(20)	6	(35)*,†
6q22	26	(36)	4	(27)	22	(39)	14	(35)	8	(47)
7p21-p22	6	(8)	1	(7)	5	(9)	3	(8)	2	(12)
7p15	6	(8)	1	(7)	5	(9)	3	(8)	2	(12)
7q11	8	(11)	3	(20)	5	(9)	3	(8)	2	(12)
7q31-q32	8	(11)	3	(20)	5	(9)	2	(5)	3	(18)
7q33-q35	8	(11)	3	(20)	5	(9)	2	(5)	3	(18)
7q36	8	(11)	3	(20)	5	(9)	2	(5)	3	(18)
8p22-p23	31	(43)	4	(27)	27	(47)	19	(48)	8	(47)
8p21	31	(43)	4	(27)	27	(47)	20	(50)	7	(41)
8q11	27	(38)	3	(20)	24	(42)	17	(43)	7	(41)
9p22	33	(46)	4	(27)	29	(51)	19	(48)	[redacted]	
9q12-q13	28	(39)	3	(20)	25	(44)	16	(40)	9	(53)
10p13-p14	12	(17)	2	(13)	10	(18)	6	(15)	4	(24)
10p12-p13	12	(17)	3	(20)	9	(16)	6	(15)	3	(18)
10p12	12	(17)	3	(20)	9	(16)	7	(18)	2	(12)
10p11	12	(17)	3	(20)	9	(16)	7	(18)	2	(12)
10q25-q26	16	(22)	4	(27)	12	(21)	9	(23)	3	(18)
11p12	16	(22)	0	(0)	16	(28)*,†	10	(25)*,†	6	(35)*
11p11-p12	16	(22)	0	(0)	16	(28)*,†	9	(23)	7	(41)†
11q24-q25	21	(29)	1	(7)	20	(35)*,†	15	(38)*,†	5	(29)
12p12-p13	24	(33)	2	(13)	22	(39)	16	(40)	6	(35)
12q11-q12	21	(29)	1	(7)	20	(35)	14	(35)*,†	6	(35)
13q13	[redacted]		[redacted]		[redacted]		[redacted]		8	(47)
14q21	14	(19)	1	(7)	13	(23)	7	(18)	6	(35)
15q14-q21	23	(32)	1	(7)	22	(39)*,†	16	(40)*,†	6	(35)
16p11	11	(15)	0	(0)	11	(19)	9	(23)	2	(12)
16q22	18	(25)	1	(7)	17	(30)	13	(33)	4	(24)
16q23-q24	18	(25)	1	(7)	17	(30)	13	(33)	4	(24)
17p12-p13	[redacted]		2	(13)	[redacted]†		[redacted]†		[redacted]†	

(Continued on the following page)

Table 2. Frequency of AI on each chromosome arm in small-sized lung adenocarcinomas (Cont'd)

Chromosomal regions with AI	No. of cases (%)									
	Total		Subtype							
			Noninvasive		Invasive					
			A + B		All		C		D	
	n = 72		n = 15		n = 57		n = 40		n = 17	
17q11	32	(44)	2	(13)	30	(53)†	21	(53)*	9	(53)*
18p11	24	(33)	1	(7)	23	(40)*	18	(45)†	5	(29)
18q21	30	(42)	4	(27)	26	(46)	19	(48)	7	(41)
19p12-p13	20	(28)	4	(27)	16	(28)	10	(25)	6	(35)
19q12	20	(28)	4	(27)	16	(28)	10	(25)	6	(35)
20p11	20	(28)	1	(7)	19	(33)	15	(38)*	4	(24)
20q11	19	(26)	1	(7)	18	(32)	14	(35)*	4	(24)
21q11-q21	13	(18)	0	(0)	13	(23)	9	(23)	4	(24)
22q12	18	(25)	1	(7)	17	(30)	10	(25)	7	(41)*

NOTE: Frequency > mean + SD is marked by yellow, and frequency > mean + 2SD is marked by red.
*P < 0.05 for the difference against noninvasive tumors by Fischer's exact test.
†P < 0.01 for the difference against noninvasive tumors by Fischer's exact test.

(P < 0.05; Table 3). In particular, AI at 8p21 was also significantly more frequently detected in cases with poor prognosis than in cases with good prognosis (P = 0.046; Table 3). AIs of the other 51 regions as well as *EGFR*, *KRAS*, and *TP53* mutations were not associated with prognosis. The log-rank test also indicated that overall survival of cases with AI at 8p21 is worse than that without (Fig. 1; P = 0.036). Because 8p21 was defined as a hotspot of AI in both noninvasive and invasive tumors, AI at 8p21 was suggested to occur early in the development of adenocarcinoma. Therefore, it is possible that adenocarcinomas with AI at 8p21 are more aggressive than those without, even if the sizes of tumors are small. The result may indicate that AI at 8p21 could be a prognostic marker of small-sized adenocarcinomas.

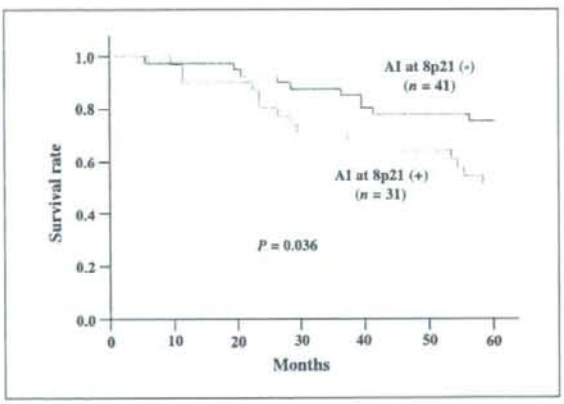

Figure 1. Prognostic significance of AI at 8p21 in patients with small-sized lung adenocarcinoma. Overall survival of patients with and without AI were compared by Kaplan-Meier curves and the log-rank test (P = 0.036).

Association of AIs with *EGFR/KRAS* mutations, gender, and smoking history. It is known that *EGFR* mutations are frequently detected in adenocarcinomas in female nonsmokers, whereas *KRAS* mutations are in adenocarcinomas in male smokers (25, 26). Such an association was also detected in this study (Supplementary Table S3). Therefore, it is important to examine whether any AIs occur in association with *EGFR/KRAS* mutations, gender, or smoking. The 72 tumors were subdivided into three groups according to the status of *EGFR/KRAS* mutations: 40 (56%) tumors with *EGFR* mutations, 8 (11%) tumors with *KRAS* mutations, and 24 (33%) tumors without *EGFR/KRAS* mutations (Table 1). Among the 52 AI regions, only 2 regions were significantly differentially affected among the three groups. 4q13 and 4q22 were more frequently affected in tumors with *EGFR* mutations than in those without *EGFR/KRAS* mutations (Supplementary Table S2). We also evaluated the association of genetic alterations with gender and smoking history. AI at 1p21-p22, 1p13-p21, and 9p22 was detected predominantly in female patients, and AI at 19p12-p13 was in smokers (Supplementary Table S3).

Genetic model for the development of lung adenocarcinoma. Based on the results, a genetic model for the development of lung adenocarcinoma was constructed (Fig. 2). Mutually exclusive *EGFR* or *KRAS* mutations were detected in the majority of type A and type B tumors, and the frequency of *EGFR/KRAS* mutations in type A and type B tumors was similar to that in type C tumors. Therefore, it is likely that type A and type B noninvasive tumors with *EGFR* or *KRAS* mutations progress to type C invasive tumors by acquisition of additional genetic alterations. A subset of type A and type B tumors had neither *EGFR* nor *KRAS* mutation and, thus, may also progress to type C invasive tumors without acquiring *EGFR* and *KRAS* mutations. The frequency of *KRAS* mutations in type D tumors was similar to those in replacement growth type (types A, B, and C) tumors, whereas the

Table 3. Correlation of genetic alterations with pathologic stage and prognosis in small-sized lung adenocarcinomas

Genetic alteration	No. of cases (%)							
	Pathologic stage				Prognosis*			
	IA		>IA		Alive		Dead	
	(n = 41)		(n = 31)		(n = 47)		(n = 25)	
Allelic imbalance								
1p21-p22	7	(17)	6	(19)	8	(17)	5	(20)
1p13-p21	7	(17)	6	(19)	8	(17)	5	(20)
1q21	8	(20)	5	(16)	8	(17)	5	(20)
2p22-p24	6	(15)	5	(16)	8	(17)	3	(12)
2q35-q37	6	(15)	6	(19)	7	(15)	5	(20)
3p14	10	(24)	14	(45)	17	(36)	7	(28)
3q11	12	(29)	10	(32)	18	(38)	5	(20)
4p12-p13	5	(12)	6	(19)	7	(15)	4	(16)
4q13	10	(24)	7	(23)	11	(23)	6	(24)
4q22	11	(27)	6	(19)	11	(23)	6	(24)
5p15	4	(10)	6	(19)	4	(9)	6	(24)
5p12-p13	5	(12)	5	(16)	6	(13)	4	(16)
5q23	12	(29)	11	(35)	14	(30)	9	(36)
6p11	3	(7)	11†	(35)	7	(15)	7	(28)
6q22	12	(29)	14	(45)	15	(32)	11	(44)
7p21-p22	1	(2)	5	(16)	4	(9)	2	(8)
7p15	1	(2)	5	(16)	4	(9)	2	(8)
7q11	3	(7)	5	(16)	6	(13)	2	(8)
7q31-q32	3	(7)	5	(16)	7	(15)	1	(4)
7q33-q35	3	(7)	5	(16)	7	(15)	1	(4)
7q36	4	(10)	4	(13)	6	(13)	2	(8)
8p22-p23	12	(29)	19†	(61)	17	(36)	14†	(56)
8p21	12	(29)	19†	(61)	16	(34)	15†	(60)
8q11	11	(27)	16†	(52)	15	(32)	12	(48)
9p22	16	(39)	17	(55)	19	(40)	14	(56)
9q12-q13	14	(34)	14	(45)	16	(34)	12	(48)
10p13-p14	6	(15)	6	(19)	9	(19)	3	(12)
10p12-p13	6	(15)	6	(19)	9	(19)	3	(12)
10p12	5	(12)	7	(23)	9	(19)	3	(12)
10p11	5	(12)	7	(23)	9	(19)	3	(12)
10q25-q26	6	(15)	10	(32)	12	(26)	4	(16)
11p12	4	(10)	12†	(39)	7	(15)	9	(36)
11p11-p12	5	(12)	11†	(35)	8	(17)	8	(32)
11q24-q25	8	(20)	13	(42)	13	(28)	8	(32)
12p12-p13	10	(24)	14	(45)	12	(26)	12	(48)
12q11-q12	9	(22)	12	(39)	10	(21)	11	(44)
13q13	23	(56)	19	(61)	26	(55)	16	(64)
14q21	6	(15)	8	(26)	11	(23)	3	(12)
15q14-q21	10	(24)	13	(42)	13	(28)	10	(40)
16p11	4	(10)	7	(23)	5	(11)	6	(24)
16q22	6	(15)	12†	(39)	9	(19)	9	(36)
16q23-q24	6	(15)	12†	(39)	9	(19)	9	(36)
17p12-p13	17	(41)	23†	(74)	25	(53)	15	(60)
17q11	15	(37)	17	(55)	19	(40)	13	(52)
18p11	10	(24)	14	(45)	13	(28)	11	(44)
18q21	14	(34)	16	(52)	19	(40)	11	(44)
19p12-p13	11	(27)	9	(29)	12	(26)	8	(32)
19q12	11	(27)	9	(29)	13	(28)	7	(28)
20p11	8	(20)	12	(39)	10	(21)	10	(40)
20q11	8	(20)	11	(35)	10	(21)	9	(36)
21q11-q21	6	(15)	7	(23)	6	(13)	7	(28)
22q12	7	(17)	11	(35)	9	(19)	9	(36)

(*Continued on the following page*)

Table 3. Correlation of genetic alterations with pathologic stage and prognosis in small-sized lung adenocarcinomas (Cont'd)

Genetic alteration	No. of cases (%)							
	Pathologic stage				Prognosis*			
	IA		>IA		Alive		Dead	
	(n = 41)		(n = 31)		(n = 47)		(n = 25)	
Mutation								
EGFR	23	(56)	17	(55)	24	(51)	16	(64)
KRAS	6	(15)	2	(6)	6	(13)	2	(8)
TP53	18	(44)	19	(61)	21	(45)	16	(64)

* Postoperative 5-y overall survival.
† $P < 0.05$ by Fischer's exact test.

frequency of *EGFR* mutations in type D tumors was much lower than those in replacement growth type tumors. These results strongly indicate that the majority of type D tumors are generated through a pathway(s) distinct from replacement growth type tumors without *EGFR/KRAS* mutations (14), and a subset of type D tumors are progressed from type C tumors, in particular, with *KRAS* mutations.

AI of 13q13 was observed frequently in both noninvasive and invasive tumors, and with similar frequencies in replacement and nonreplacement growth types and among three groups according to the status of *EGFR/KRAS* mutations (Supplementary Table S2). Therefore, 13q13 alterations were suggested to contribute to the formation of noninvasive tumors irrespective of *EGFR/KRAS* mutation. We recently reported that *p16* homozygous deletions also occur with similar frequencies (~25%) in noninvasive and invasive tumors, in replacement and nonreplacement growth types, and among three groups according to the status of *EGFR/KRAS* mutations (8). The *p16* gene is located on chromosome 9p, which was a hotspot/critical region of AI in both noninvasive and invasive tumors. Therefore, *p16* inactivation would also be an early genetic event as 13q13 alterations are.

AI of 17p12-p13 as well as *TP53* mutations was observed frequently in invasive tumors, particularly in type D tumors, and commonly among three groups for *EGFR/KRAS* mutations (Table 1; Supplementary Table S2). There was a significant association between *TP53* mutations and AI of 17p12-p13 (P = 0.0007) in the tumors. Therefore, the *TP53* gene was inactivated by these two-hit alterations in the majority of tumors analyzed. The result indicated that *TP53* inactivation contributes to the progression of

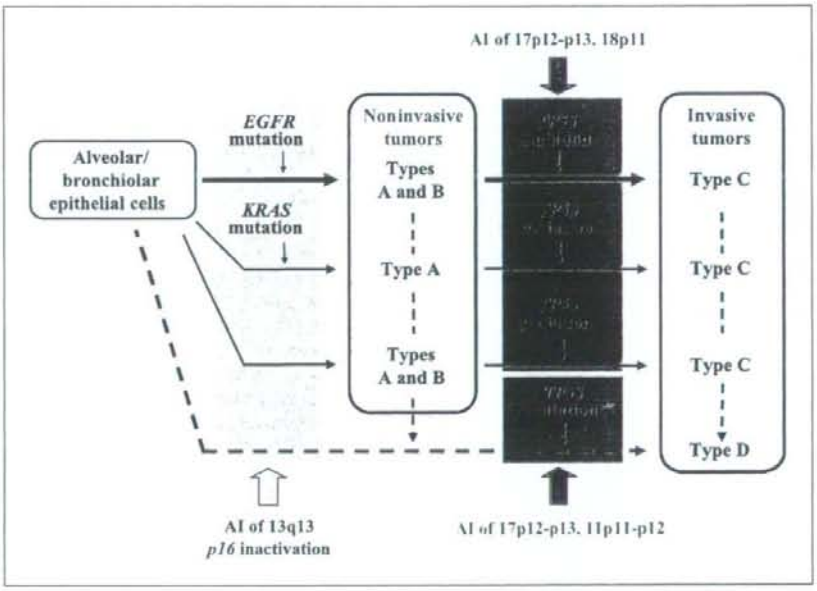

Figure 2. A genetic model for progression of small-sized lung adenocarcinoma. *EGFR* or *KRAS* mutations, AI of 13q13, and *p16* inactivation are genetic alterations for the development of type A and type B tumors, and they progress to type C tumors by acquiring *TP53* mutations and AIs of 17p12-p13/18p11. Because *KRAS* mutations were infrequent in type B tumors, tumors with *KRAS* mutations could rapidly progress from type A to type C tumors. A subset of type A, B, or C tumors do not have *EGFR/KRAS* mutations and, thus, are developed through a pathway other than the *EGFR/KRAS* pathways. Type D, nonreplacement growth type tumor, can either arise *de novo* or progress from some replacement growth type tumors by acquiring *p16* inactivation, *TP53* mutations, and AIs of 13q13, 17p12-p13, and 11p11-p12.

noninvasive tumors to invasive ones, irrespective of *EGFR/KRAS* mutation. Because frequencies of AI of 18p11 and 11p11-p12 in type C and type D tumors, respectively, against those in noninvasive tumors were significantly high ($P < 0.01$; Table 2), AI of 18p11 is likely to be involved in the progression of replacement type growth tumors, whereas AI of 11p11-p12 may contribute to the development of type D tumors.

Confirmation of AI at 8p21 by microsatellite analysis. To confirm the presence of AI at 8p21 detected by 10K array analysis, microsatellite analysis was done against two microsatellite markers, *D8S1116* and *D8S322*, mapped in the common region of AI at 8p21 (Supplementary Fig. S1). Among 72 cases subjected to 10K array analysis, DNA was available in 61 cases for the microsatellite analysis. Fifty-one of the 61 cases were informative (heterozygous for either *D8S1116* or *D8S322*), and the frequency of AI by microsatellite analysis (29 of 51, 57%) was slightly higher than that by 10K array analysis (23 of 51, 45%). However, the concordance of the results between microsatellite analysis and 10K array analysis was highly significant ($P < 0.0001$), and AI at 8p21 determined by microsatellite analysis was also significantly more frequently detected in cases with poor prognosis than cases with good prognosis (10 of 12 versus 19 of 39, $P = 0.0475$). Therefore, AI detected by 10K array analysis was confirmed by microsatellite analysis. To validate the prognostic significance of AI at 8p21, newly microdissected 40 cases were further subjected to microsatellite analysis. Thirty-eight of them were informative, and, in total of 89 informative cases, AI at 8p21 in cases with poor prognosis (22 of 29, 76%) was significantly higher than that in cases with good prognosis (30 of 60, 50%; $P = 0.0234$).

Discussion

We undertook a genome-wide comparative analysis of AI as well as mutational analysis of the *EGFR/KRAS/TP53* genes between noninvasive and invasive small-sized lung adenocarcinomas. *EGFR* and *KRAS* mutations were detected at similar frequencies between noninvasive and invasive tumors, whereas the frequency of *TP53* mutations in invasive tumors was significantly higher than that in noninvasive ones (Table 1). The number of AI regions in invasive tumors was significantly higher than that in noninvasive ones. There were 12 regions whose frequencies of AI were significantly higher in invasive tumors than in noninvasive ones, whereas there were no regions whose frequencies of AI were significantly higher vice versa (Table 2). The results indicated that noninvasive tumors progress to invasive ones by further inactivation of several tumor suppressor genes. A genetic model for the progression of small-sized lung adenocarcinoma constructed based on the results of this study went along well with the progression model deduced from the histopathologic findings (15); type A tumors progress sequentially through type B to type C tumors, whereas the majority of type D tumors are generated through a pathway distinct from type C tumors. *EGFR* or *KRAS* mutations and AI at 13q13, in addition to *p16* inactivation, contribute to the development of type A and type B noninvasive tumors, whereas *p53* mutation and AIs of 17p12-p13 and 18p11 contribute to their progression to type C invasive tumors. On the other hand, most type D tumors do not have *EGFR* or *KRAS* mutations and, therefore, are generated through a pathway distinct from that of type C tumors. A small subset of type D tumors carried *EGFR* or *KRAS* mutations and, therefore, could be developed from type A and type B noninvasive tumors, but these tumors rapidly progressed to invasive ones.

Importantly, AI at 13q13 was frequent not only in replacement growth types but also in nonreplacement growth types. Therefore, it is a common event in adenocarcinoma irrespective of growth types. AI at 13q has been defined as a frequent genetic alteration in non–small-cell lung cancer (9, 10). *RB1* is a tumor suppressor gene located at 13q14 that is frequently inactivated in small-cell lung carcinoma. However, *RB1* inactivation is infrequent in non–small-cell lung cancer (27, 28) and, therefore, *RB1* is unlikely to be a target for AI in adenocarcinoma. Consistently, the 13q13 region defined as a common region of AI in this study did not include the *RB1* gene. Thus, a gene(s) other than *RB1* is likely to function as a tumor suppressor.

17p12-p13 is the most common region of AIs in invasive tumors, in particular in type D tumors. It was shown in our present and previous studies that the *TP53* gene is preferentially mutated in invasive tumors among small-sized adenocarcinomas (6, 8), and the *TP53* gene was mapped in the common region of AIs on 17p in this study. Therefore, *TP53* inactivation due to a mutation of one allele and a loss of the other allele is likely to contribute to the progression of noninvasive tumors to invasive ones. The frequency of *TP53* mutations in invasive tumors, particularly in type D (82%), was extremely high in this study. A major reason of such a high frequency would be the use of microdissected materials for the analysis to avoid overlooking of mutations. In addition, type C cases with poor prognosis and poorly differentiated type D cases were intentionally selected as invasive tumors. Therefore, a majority of the cases were males, smokers, and in advanced stages (>IA). *TP53* mutations were more frequently detected in these subsets, although the difference in each subset was not statistically significant (Table 3; Supplementary Table S3). The results strongly indicate that *TP53* mutations are predominantly accumulated in advanced stage invasive tumors of male smokers.

The 11p12-p13 region possibly contains a tumor suppressor gene involved in the formation of type D tumors. We recently reported that AI at 11p11-p12 is frequently accumulated in brain metastases of lung cancer (21); therefore, this region might contain a gene(s) involved in the invasion and metastasis of adenocarcinoma cells. The 18p11 region possibly contains a tumor suppressor gene involved in the formation of type C tumors. In addition, AIs at 4q13 and 4q22 were significantly more frequent in *EGFR* type tumors than in non-*EGFR/KRAS* type tumors. Therefore, it is likely that these AIs are also involved in the development and/or progression of adenocarcinoma in genetic pathway– and progression stage–specific manners.

Patients with AI at 8p21 in tumors showed worse prognoses than those without. Therefore, AI at 8p21 would also be involved in invasion and metastasis of adenocarcinoma cells and be a useful marker for the prognosis of patients with small-sized lung adenocarcinoma. It was reported that AI at 8p is present in premalignant epithelium of the lung as well as in adenocarcinomas (29, 30), and these findings were confirmed in this study. 8p21 was a hotspot of AIs both in noninvasive and invasive tumors; therefore, AI at 8p21 might enhance metastatic potentials of tumor cells at any developmental stages. AI on 8p was reported to occur frequently in several types of cancers, including hepatocellular carcinoma, prostate cancer, and breast cancer, and its correlation with poor prognosis was also observed in these cancers (31–34). Thus, AI on 8p could be useful for the

prediction of prognosis of patients with small-sized lung adenocarcinoma as well as several other cancers. Although a target gene(s) on 8p is unknown at present, 37 genes, including *TNFRSF10B/TRAIL-R2* and *LZTS1/FEZ1* candidate tumor suppressors (35–37), were mapped in the 8p21 AI regions (Supplementary Table S1). Therefore, mutational and expression analyses of these genes are in progress.

AIs associated with other clinicopathologic factors were also identified at several chromosomal regions. There were nine regions more frequently affected in stage >IA tumors than in stage IA tumors ($P < 0.05$; Table 3). Therefore, genes in these regions might also contribute to invasion and/or metastasis of adenocarcinoma cells. AI at 19p12-p13 was detected more frequently in smokers than in nonsmokers (Supplementary Table S3). This result was consistent with our recent report that the *LKB1* gene at 19p13 is inactivated preferentially in lung cancers of smokers (38) and, therefore, indicates that *LKB1* is a target tumor suppressor for 19p AI. In addition, AIs of 1p21-p22, 1p13-p21, and 9p22 were detected predominantly in female patients; therefore, these regions might contain tumor suppressors whose inactivation preferentially contributes to the development of adenocarcinomas in females that are different from those in males in several aspects (25, 26). Further molecular analyses with more cases of small-sized adenocarcinoma will be necessary to validate the roles of these genetic alterations. Identification of target genes will also facilitate the understanding of multistep carcinogenic pathways of lung adenocarcinoma.

Disclosure of Potential Conflicts of Interest

No potential conflicts of interest were disclosed.

Acknowledgments

Received 8/20/2008; revised 10/20/2008; accepted 11/19/2008; published OnlineFirst 02/03/2009.

Grant support: Grants-in-Aid from the Ministry of Health, Labor and Welfare for the 3rd-Term Comprehensive 10-Year Strategy for Cancer Control and for Cancer Research (16-1) and from the Program for Promotion of Fundamental Studies in Health Sciences of the National Institute of Biomedical Innovation (NiBio).

The costs of publication of this article were defrayed in part by the payment of page charges. This article must therefore be hereby marked *advertisement* in accordance with 18 U.S.C. Section 1734 solely to indicate this fact.

References

1. Travis WD, Brambilla E, Muller-Hermelink HK, Harris CC. World Health Organization classification of tumors: pathology and genetics, tumours of lung, pleura, thymus and heart. Lyon: IARC Press; 2004.
2. Adjei AA. Blocking oncogenic Ras signaling for cancer therapy. J Natl Cancer Inst 2001;93:1062–74.
3. Lynch TJ, Bell DW, Sordella R, et al. Activating mutations in the epidermal growth factor receptor underlying responsiveness of non-small-cell lung cancer to gefitinib. N Engl J Med 2004;350:2129–39.
4. Paez JG, Janne PA, Lee JC, et al. EGFR mutations in lung cancer: correlation with clinical response to gefitinib therapy. Science 2004;304:1497–500.
5. Shigematsu H, Lin L, Takahashi T, et al. Clinical and biological features associated with epidermal growth factor receptor gene mutations in lung cancers. J Natl Cancer Inst 2005;97:339–46.
6. Matsumoto S, Iwakawa R, Kohno T, et al. Frequent EGFR mutations in noninvasive bronchioloalveolar carcinoma. Int J Cancer 2006;118:2498–504.
7. Sakamoto H, Shimizu J, Horio Y, et al. Disproportionate representation of KRAS gene mutation in atypical adenomatous hyperplasia, but even distribution of EGFR gene mutation from preinvasive to invasive adenocarcinomas. J Pathol 2007;212:287–94.
8. Iwakawa R, Kohno T, Anami Y, et al. Association of p16 homozygous deletions with clinicopathological characteristics and EGFR/KRAS/p53 mutations in lung adenocarcinoma. Clin Cancer Res 2008;14:3746–53.
9. Shiseki M, Kohno T, Adachi J, et al. Comparative allelotype of early and advanced stage non-small cell lung carcinomas. Genes Chromosomes Cancer 1996;17:71–7.
10. Shiseki M, Kohno T, Nishikawa R, Sameshima Y, Mizoguchi H, Yokota J. Frequent allelic losses on chromosomes 2q, 18q, and 22q in advanced non-small cell lung carcinoma. Cancer Res 1994;54:5643–8.
11. Tsuchiya E, Nakamura Y, Weng SY, et al. Allelotype of non-small cell lung carcinoma—comparison between loss of heterozygosity in squamous cell carcinoma and adenocarcinoma. Cancer Res 1992;52:2478–81.
12. Zhao X, Li C, Paez JG, et al. An integrated view of copy number and allelic alterations in the cancer genome using single nucleotide polymorphism arrays. Cancer Res 2004;64:3060–71.
13. Virmani AK, Fong KM, Kodagoda D, et al. Allelotyping demonstrates common and distinct patterns of chromosomal loss in human lung cancer types. Genes Chromosomes Cancer 1998;21:308–19.
14. Girard L, Zochbauer-Muller S, Virmani AK, Gazdar AF, Minna JD. Genome-wide allelotyping of lung cancer identifies new regions of allelic loss, differences between small cell lung cancer and non-small cell lung cancer, and loci clustering. Cancer Res 2000;60:4894–906.
15. Noguchi M, Morikawa A, Kawasaki M, et al. Small adenocarcinoma of the lung. Histologic characteristics and prognosis. Cancer 1995;75:2844–52.
16. Henschke CI, Yankelevitz DF, Libby DM, Pasmantier MW, Smith JP, Miettinen OS. Survival of patients with stage I lung cancer detected on CT screening. N Engl J Med 2006;355:1763–71.
17. Travis WD, Garg K, Franklin WA, et al. Bronchioloalveolar carcinoma and lung adenocarcinoma: the clinical importance and research relevance of the 2004 World Health Organization pathologic criteria. J Thorac Oncol 2006;1:S13–9.
18. Goldstraw P, Crowley J, Chansky K, et al. The IASLC Lung Cancer Staging Project: proposals for the revision of the TNM stage groupings in the forthcoming (seventh) edition of the TNM Classification of malignant tumours. J Thorac Oncol 2007;2:706–14.
19. Aoyagi Y, Yokose T, Minami Y, et al. Accumulation of losses of heterozygosity and multistep carcinogenesis in pulmonary adenocarcinoma. Cancer Res 2001;61:7950–4.
20. Soblin LHW, editor. TNM classification of malignant tumors. 6th ed. New York: Wiley-Liss; 2002. p. 99–103.
21. Takahashi K, Kohno T, Matsumoto S, et al. Clonal and parallel evolution of primary lung cancers and their metastases revealed by molecular dissection of cancer cells. Clin Cancer Res 2007;13:111–20.
22. Ogiwara H, Kohno T, Nakanishi H, Nagayama K, Sato M, Yokota J. Unbalanced translocation, a major chromosome alteration causing loss of heterozygosity in human lung cancer. Oncogene 2008;27:4788–97.
23. Kosaka T, Yatabe Y, Endoh H, Kuwano H, Takahashi T, Mitsudomi T. Mutations of the epidermal growth factor receptor gene in lung cancer: biological and clinical implications. Cancer Res 2004;64:8919–23.
24. Eberhard DA, Johnson BE, Amler LC, et al. Mutations in the epidermal growth factor receptor and in KRAS are predictive and prognostic indicators in patients with non-small-cell lung cancer treated with chemotherapy alone and in combination with erlotinib. J Clin Oncol 2005;23:5900–9.
25. Sun S, Schiller JH, Gazdar AF. Lung cancer in never smokers—a different disease. Nat Rev Cancer 2007;7:778–90.
26. Toyooka S, Tokumo M, Shigematsu H, et al. Mutational and epigenetic evidence for independent pathways for lung adenocarcinomas arising in smokers and never smokers. Cancer Res 2006;66:1371–5.
27. Yokota J, Kohno T. Molecular footprints of human lung cancer progression. Cancer Sci 2004;95:197–204.
28. Tamura K, Zhang X, Murakami Y, et al. Deletion of three distinct regions on chromosome 13q in human non-small-cell lung cancer. Int J Cancer 1997;74:45–9.
29. Wistuba II, Behrens C, Virmani AK, et al. Allelic losses at chromosome 8p21-23 are early and frequent events in the pathogenesis of lung cancer. Cancer Res 1999;59:1973–9.
30. Emi M, Fujiwara Y, Nakajima T, et al. Frequent loss of heterozygosity for loci on chromosome 8p in hepatocellular carcinoma, colorectal cancer, and lung cancer. Cancer Res 1992;52:5368–72.
31. Emi M, Fujiwara Y, Ohata H, et al. Allelic loss at chromosome band 8p21.3-p22 is associated with progression of hepatocellular carcinoma. Genes Chromosomes Cancer 1993;7:152–7.
32. Jenkins R, Takahashi S, DeLacey K, Bergstralh E, Lieber M. Prognostic significance of allelic imbalance of chromosome arms 7q, 8p, 16q, and 18q in stage T3N0M0 prostate cancer. Genes Chromosomes Cancer 1998;21:131–43.
33. Sigbjornsdottir BI, Ragnarsson G, Agnarsson BA, et al. Chromosome 8p alterations in sporadic and BRCA2 999del5 linked breast cancer. J Med Genet 2000;37:342–7.
34. Zhou W, Goodman M, Lyles RH, et al. Surgical margin and Gleason score as predictors of postoperative recurrence in prostate cancer with or without chromosome 8p allelic imbalance. Prostate 2004;61:81–91.
35. Lee SH, Shin MS, Kim HS, et al. Alterations of the DR5/TRAIL receptor 2 gene in non-small cell lung cancers. Cancer Res 1999;59:5683–6.
36. Toyooka S, Fukuyama Y, Wistuba II, Tockman MS, Minna JD, Gazdar AF. Differential expression of FEZ1/LZTS1 gene in lung cancers and their cell cultures. Clin Cancer Res 2002;8:2292–7.
37. Nonaka D, Fabbri A, Roz L, et al. Reduced FEZ1/LZTS1 expression and outcome prediction in lung cancer. Cancer Res 2005;65:1207–12.
38. Matsumoto S, Iwakawa R, Takahashi K, et al. Prevalence and specificity of LKB1 genetic alterations in lung cancers. Oncogene 2007;26:5911–8.

Modern Pathology (2007) 20, 215–220

www.modernpathology.org

Immunohistochemical detection of GLUT-1 can discriminate between reactive mesothelium and malignant mesothelioma

Yasufumi Kato[1,2], Koji Tsuta[1], Kunihiko Seki[1], Akiko Miyagi Maeshima[3], Shunichi Watanabe[2], Kenji Suzuki[2], Hisao Asamura[2], Ryosuke Tsuchiya[2] and Yoshihiro Matsuno[1]

[1]*Clinical Laboratory, National Cancer Center Hospital, Tokyo, Japan;* [2]*Thoracic Surgery Divisions, National Cancer Center Hospital, Tokyo, Japan and* [3]*Pathology Division, National Cancer Center Research Institute, Tokyo, Japan*

The separation of benign reactive mesothelium (RM) from malignant mesothelial proliferation can be a major challenge. A number of markers have been proposed, including epithelial membrane antigen, p53 protein, and P-glycoprotein. To date, however, no immunohistochemical marker that allows unequivocal discrimination of RM from malignant pleural mesothelioma (MPM) has been available. A family of glucose transporter isoforms (GLUT), of which GLUT-1 is a member, facilitate the entry of glucose into cells. GLUT-1 is largely undetectable by immunohistochemistry in normal epithelial tissues and benign tumors, but is expressed in a variety of malignancies. Thus, the expression of GLUT-1 appears to be a potential marker of malignant transformation. Recently, in fact, some studies have shown that GLUT-1 expression is useful for distinguishing benign from malignant lesions. The purpose of the present study was to evaluate the diagnostic utility of GLUT-1 expression for diagnostic differentiation between RM and MPM. Immunohistochemical staining for GLUT-1 was performed in 40 cases of RM, 48 cases of MPM, and 58 cases of lung carcinoma. Immunohistochemical GLUT-1 expression was seen in 40 of 40 (100%) MPMs, and in all cases the expression was demonstrated by linear plasma membrane staining, sometimes with cytoplasmic staining in addition. GLUT-1 expression was also observed in 56 out of 58 (96.5%) lung carcinomas. On the other hand, no RM cases were positive for GLUT-1. GLUT-1 is a sensitive and specific immunohistochemical marker enabling differential diagnosis of RM from MPM, whereas it cannot discriminate MPM from lung carcinoma.
Modern Pathology (2007) **20,** 215–220. doi:10.1038/modpathol.3800732; published online 22 December 2006

Keywords: Glut-1; reactive methothelium; malignant pleural mesothelioma; immunohistochemistry; lung carcinoma

The separation of benign reactive mesothelium (RM) from malignant mesothelial proliferation can be a major challenge. The common cytomorphological features associated with malignancy, such as high cellularity/proliferation, marked cytonuclear atypia and high mitotic rate are of very limited use in this setting. Thus, it is sometimes very difficult, or almost impossible even for expert pathologists to make a definite diagnosis of malignant mesothelioma, especially in small specimens, unless there is unequivocal invasion of adjacent tissues by tumor cells.[1] On the other hand, early diagnosis of malignant pleural mesothelioma (MPM) in small closed pleural biopsy samples, or by cytology, is crucial for patient management and may facilitate the avoidance of invasive surgical procedures.

A number of immunohistochemical markers have been proposed to assist conventional morphological diagnosis, including epithelial membrane antigen (EMA)[2–5] p53 protein,[2–11] and P-glycoprotein.[2,5,12] Other markers tested have included Bcl-2,[2,3,13] platelet-derived growth factor receptor (PDGF-R) β-chain[2,5,8] and desmin.[2] To date, however, no single immunohistochemical marker that can unequivocally discriminate RM from MPM has been available.

GLUT-1 is one of 14 members of the mammalian facilitative glucose transporter (GLUT) family of passive carriers that function as an energy-independent system for transport of glucose down a concentration gradient.[14] GLUT-1 is not detectable

Correspondence: Dr Y Matsuno, MD, Clinical Laboratory Division, National Cancer Center Hospital, 1-1, Tsukiji 5-chome, Chuo-ku, Tokyo 104-0045, Japan.
E-mail: ymatsuno@ncc.go.jp
Received 30 August 2006; accepted 23 October 2006; published online 22 December 2006

in a large proportion of cells from normal tissues and benign lesions, except for erythrocytes, germinal cells of the testis, renal tubules, perineurium of peripheral nerves, endothelial cells in blood–brain barrier vessels, and placenta (trophoblasts and capillaries).[15,16] In contrast, GLUT-1 is expressed in a variety of carcinomas such as those of the breast, head and neck, bladder, renal cells, and lung.[15–24] Previous reports suggest that the expression of GLUT-1 may be a potential marker for malignancy.

Recently, some studies have shown that GLUT-1 expression is useful for resolving the common diagnostic dilemma of distinguishing benign from malignant lesions.[25,26] Although a few studies have demonstrated that GLUT-1 is useful for distinguishing RM from metastatic adenocarcinoma in body cavity effusions,[27–29] the study cohorts did not include MPM. Using immunohistochemistry, Godoy *et al*[16] analyzed coexpression of GLUT-1 and other GLUT isoforms (GLUT-2 to -6 and GLUT-9) in a variety of benign and malignant tumors, and demonstrated that two of four MPMs were positive for GLUT-1. However, they did not analyze reactive and normal mesothelium.

The purpose of the present study was to evaluate the diagnostic utility of GLUT-1 detection for differential diagnosis between RM and MPM.

Materials and methods

Case Selection

The materials for the present study were extracted from cases deposited in the pathology files of the National Cancer Center Hospital, Tokyo, between 1971 and 2005. They comprised 40 cases of RM, 48 cases of MPM (epithelioid, 36 cases; biphasic, 11 cases; sarcomatoid, 1 case), and 58 cases of lung carcinoma (squamous cell carcinoma, 28 cases; adenocarcinoma, 30 cases). All diagnoses had been made on the basis of conventional histopathologic features evident in slide preparations stained with hematoxylin and eosin, some special stains, and immunohistochemical techniques available at that time.[30,31] In the present study, immunohistochemistry for D2-40 and calretinin was added for all cases to confirm the identity of mesothelial cells (see below).

Immunohistochemistry

For immunohistochemical staining, 5-μm-thick sections were deparaffinized and treated with 3% hydrogen peroxide for 30 min to block endogenous peroxidase activity, followed by washing in deionized water for 2–3 min. Heat-induced epitope retrieval with Target Retrieval Solution (DAKO, Carpinteria, CA, USA) was performed for GLUT-1 and calretinin. After the slides had been allowed to cool at room temperature for 40 min, they were rinsed with deionized water and then washed in phosphate-buffered saline for 5 min. The slides were then stained by overnight incubation with primary antibodies against GLUT-1 (1:200, polyclonal, Dako), D2-40 (1:200, clone D2-40, Signet Laboratories, Dedham, MA, USA), and calretinin (1:100, polyclonal, Zymed, San Francisco, CA, USA). Immunoreactions were detected by the labeled streptavidin–biotin method, and visualized with 3, 3′-diaminobenzidine, followed by counterstaining with hematoxylin. Appropriate positive and negative controls (red blood cells for GLUT-1) were used for each antibody. The area of GLUT-1 staining was evaluated on a sliding scale of 0 to 3+ to represent the percentage of positive cells among mesothelial cells (indicated by D2-40 and calretinin immunostain) or tumor cells (0 = <1%, 1+ = 1–25%, 2+ = 26–50%, 3+ = >51%). Immunohistochemical staining was scored independently by two observers (YK and KT).

Results

The results of immunohistochemistry are summarized in Table 1. GLUT-1 expression was demonstrated by distinct linear plasma membrane staining, sometimes with cytoplasmic staining in addition

Table 1 Immunoreactivity of GLUT-1

	n	*GLUT-1 positive (%)*	*Staining area*			
			0	*1+*	*2+*	*3+*
Mesothelioma, all subtypes	48	48 (100)	0	15	15	18
Epithelioid	36	36 (100)	0	9	12	15
Biphasic	11	10 (90.9)[a] 7 (63.6)[b]	1[a] 4[b]	6[a] 3[b]	3[a] 2[b]	1[a] 2[b]
Sarcomatoid	1	1 (100)	0	1	0	0
Reactive mesothelium	40	0 (0)	40	0	0	0
Lung carcinoma	58	56 (96.5)	2	12	9	35
Squamous cell carcinoma	28	28 (100)	0	1	3	24
Adenocarcinoma	30	28 (93.3)	2	11	6	11

[a]Epithelioid areas.
[b]Sarcomatoid areas.

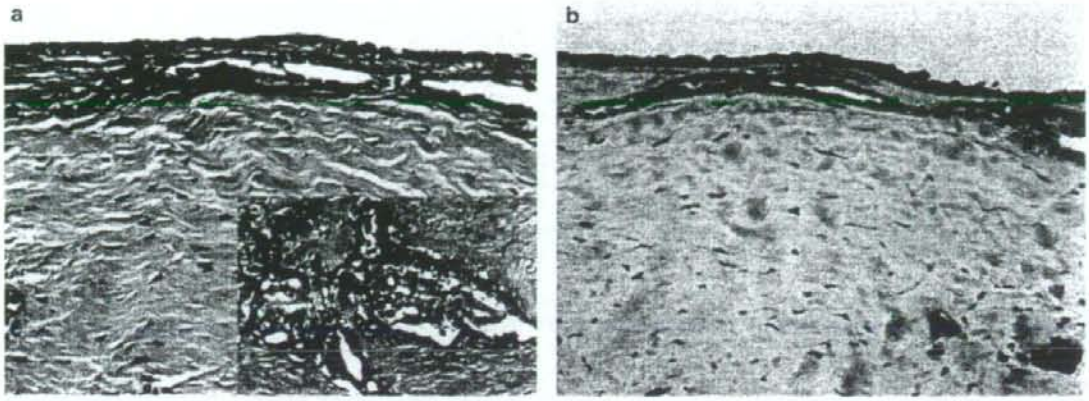

Figure 1 (**a**) In the surface area, the tumor cells showed bland cytologic atypia, nevertheless malignant mesothelioma(HE stain, × 10). Inset: the tumor cells arranged complex branching tubular formation (HE stain, × 10). (**b**) Most of the tumor cells in the epithelioid MPM were positive for GLUT-1 and red blood cells were served as internal positive control (× 10).

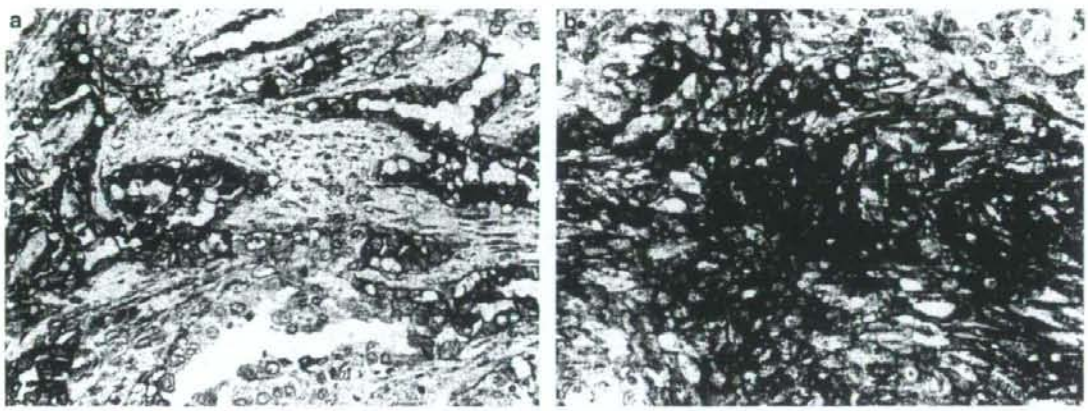

Figure 2 (**a**) More than half of the epithelioid tumor cells were positive for GLUT-1 (× 10). (**b**) Most of the sarcomatoid tumor cells were positive for GLUT-1 (× 10). The immunoreactivity was observed as distinct linear plasma membrane staining, with weak cytoplasmic staining in addition.

Table 2 GLUT-1 immunoreactivity acording to MPM histological subtype

	n	*GLUT-1-positive (%)*	*Staining area*			
			0	*1+*	*2+*	*3+*
Epithelioid area	47	46 (97.8)	1	15	15	16
Sarcomatoid area	12	8 (66.7)	4	4	2	2

(Figure 1a and b). GLUT-1 immunoreactivity was seen in 48 of 48 (100%) MPM cases, whereas no RM cases were positive for GLUT-1.

We also evaluated GLUT-1 immunoreactivity according to histological subtype, as shown in Table 2. Immunoreactivity was observed in 46 of 47 (96.7%) epithelioid mesothelioma (Figure 2a) including epithelioid areas of biphasic mesothelioma, and in seven of 12 (66.7%) sarcomatoid mesothelioma (Figure 2b) including sarcomatoid areas of biphasic mesothelioma. However, immunoreactive cells more than half of tumor cell was only 16 of 47 (34%) of epithelioid mesothelioma including epithelioid areas of biphasic mesothelioma, and two of 12 (14.1%) of sarcomatoid mesothelioma including sarcomatoid areas of biphasic mesothelioma. The GLUT-1-positive cells varied from a few cells to almost all cells in the clusters, but no characteristic staining pattern was observed in MPM.

GLUT-1 immunoreactivity was also seen in 56 of 58 (96.5%) cases of lung carcinoma. According to histological subtype, immunoreactivity was

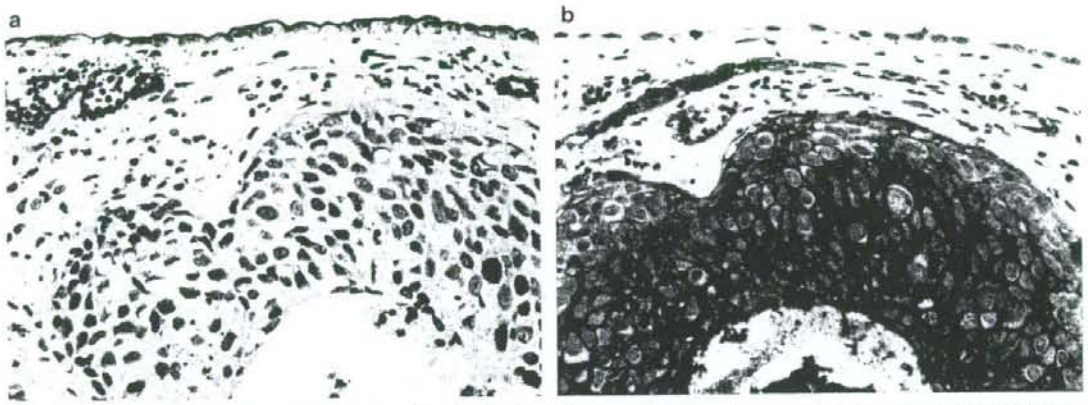

Figure 3 (**a**) D2-40 immunoreactivity was observed in the RM and lymph vessels beneath the pleura, but no immunoreactivity was observed in the poorly differentiated squamous cell carcinoma (× 10). (**b**) Most of the tumor cells without peripheral lesion in of the poorly differentiated squamous cell carcinoma were positive for GLUT-1 (red blood cells were served as internal positive control). On the other hand, RM showed no immunoreactivity for GLUT-1 (× 10).

observed in 28 of 28 (100%) cases of squamous cell carcinoma (Figure 3a and b) and 28 of 30 (93.3%) cases of adenocarcinoma. In squamous cell carcinoma, the area of positive staining was 3 + in 24 of 28 (85.7%) cases, compared with only 11 of 30 (36.7%) in cases of adenocarcinoma. Also in squamous cell carcinoma, a characteristic staining pattern was observed; tumor cells showed more intensely positive staining in the central area of tumor nests than in the peripheral area (Figure 3b).

Discussion

Morphologic differentiation between RM and MPM in small specimens can be a diagnostic challenge. The difficulty is compounded when neoplastic cells demonstrate only slight atypia. In addition, there are currently no reliable markers that allow immunohistochemical discrimination between RM and MPM. In the present study, we clearly demonstrated that GLUT-1 is a sensitive and specific immunohistochemical marker that can differentiate RM from MPM. To our knowledge, this is the first report to describe the usefulness of GLUT-1 immunostaining for discriminating between RM and MPM.

Elevated levels of expression or activation of GLUT-1, or both, have been shown to be associated with transformation of cells and malignancy, and to be modified by changes in the physiological microenvironment in tissues.[32,33] High GLUT-1 expression correlates with increased metabolism and glucose utilization in a number of normal tissues, and this transporter is overexpressed in a variety of human tumors.[15,16] Increased expression of GLUT-1 is also seen in conditions that induce greater dependency on glycolysis as an energy source, such as ischemia, hypoxia, or both.[34] These data suggest that overexpression of GLUT-1 may play an important role in the survival of tumor cells by maintaining an adequate energy supply to support their high metabolism and rapid growth in an often less-than-ideal physiological environment.[35]

GLUT-1 expression has been revealed in a variety of carcinomas, such as those of the breast, head and neck, bladder, and renal cells.[15–19,23] In the lung, about 34.3–100% of lung adenocarcinomas[16,20–22,24] and 100% of lung squamous cell carcinomas[20–22,24] are reported to express GLUT-1 at the primary site. With regard to MPM, only one article has describe that two of four studied cases were positive for GLUT-1.[16] In the present study, GLUT-1 immunoreactivity was observed in all MPMs and 56 out of 58 (96.5%) cases of lung carcinoma. These results indicate that GLUT-1 cannot discriminate between MPM and lung carcinoma. Therefore, additional appropriate positive and negative mesothelial markers are needed in order to differentiate between MPM and lung carcinoma.[31]

The heterogeneity of GLUT-1-positive areas has been reported previously. In squamous cell carcinoma, cells in the center of cancer nests, close to the necrotic area, were stained more strongly than those in peripheral areas. In adenocarcinoma, poorly differentiated areas such as the solid central area were stained more strongly than well differentiated areas such as those showing lepidic growth.[20–22,24] In the present study, more than half of all tumor cells were positive for GLUT-1 in 37.5% of MPMs, 85.7% of lung squamous cell carcinomas, and 36.7% of lung adenocarcinomas. These results indicate that GLUT-1 negativity in small samples such as those obtained by biopsy does not exclude malignancy, and that positive immunoreactivity for GLUT-1 may be an aid to accurate diagnosis of malignancy.

The GLUT-1 positivity rate in RM has been reported to be 0% (present study and Afify *et al*[29]), 3% (Zimmerman *et al*[28]), and 20% (Burstein *et al*[27]).

However, Zimmerman *et al* and Burstein *et al* reported that GLUT-1-positive cells of RM showed equivocal-to-weak staining and were easily distinguishable from unequivocal positivity of other cell types, so that the specificity of GLUT-1 was not diminished. According to them, a number of 'false-positive' cases occurred in patients with cirrhosis. The RM resulting from cirrhosis may be prompted by glucose intake to compensate for the unfavorable environment in effusion. Our cohort of RM consisted of surgically resectable cases within the physiological range or without effusion.

Positron emission tomography (PET) measurements of fluorodeoxyglucose (FDG) accumulation in different animal tumors has shown a correlation between tracer FDG uptake and the GLUT-1 mRNA content. GLUT-1 has been found to be overexpressed in tumor cells and to promote glucose metabolism and FDG accumulation in humans.[22,24] In MPM, Carretta *et al*[6] have reported that FDG-PET can differentiate RM from MPM. These findings are consistent with the present immunohistochemical results.

In summary, GLUT-1 appears to be a sensitive and specific marker for differentiating between RM and MPM, although it is unable to discriminate between MPM and lung carcinoma.

Acknowledgement

This work is supported in part by Special Coordination Funds for Promoting Science and Technology of Japan.

References

1 Allen TC, Cagle PT, Churg AM, *et al*. The separation of benign and malignant mesothelial proliferations. Am J Surg Pathol 2000;24:1183–2000.
2 Attanoos RL, Gibbs AR. Pathology of malignant mesothelioma. Histopathology 1997;30:403–418.
3 Cury PM, Butcher DN, Corrin B, *et al*. The use of histological and immunohistochemical markers to distinguish pleural malignant mesothelioma and *in situ* mesothelioma from reactive mesothelial hyperplasia and reactive pleural fibrosis. J Pathol 1999;189: 251–257.
4 Salas A, Fernandez-Banares F, Casalots J, *et al*. Utility of epithelial membrane antigen and p53 in the differential diagnosis of benign reactive processes from malignancy in pleural biopsy specimens. Virchows Arch 1999;435:286.
5 Roberts F, Harper CM, Downie I, *et al*. Immunohistochemical analysis still has a limited role in the diagnosis of malignant mesothelioma. Am J Clin Pathol 2001;116:253–262.
6 Kafiri G, Thomas DM, Shepherd NA, *et al*. p53 expression is common in malignant mesothelioma. Histopathology 1992;21:331–334.
7 Mayall FG, Goddard H, Gibbs AR. p53 immunostaining in the distinction between benign and malignant mesothelial proliferations using formalin-fixed paraffin sections. J Pathol 1992;168:377–381.
8 Ramael M, Buysse C, van den Bossche J, *et al*. Immunoreactivity for the b chain of the platelet-derived growth factor receptor in malignant mesothelioma and non-neoplastic mesothelium. J Pathol 1992; 167:1–4.
9 Ramael M, Lemmens G, Eerdekens C, *et al*. Immunoreactivity for p53 protein in malignant mesothelioma and non-neoplastic mesothelium. J Pathol 1992;168: 371–375.
10 Cagle PT, Brown RW, Lebovitz RM. p53 immunostaining in the differentiation of reactive processes from malignancy in pleural biopsy specimens. Hum Pathol 1994;25:443–448.
11 Esposito V, Baldi A, De Luca A, *et al*. p53 immunostaining in differential diagnosis of pleural mesothelial proliferations. Anticancer Res 1997;17:733–736.
12 Ramael M, van den Bossche J, Buysse C, *et al*. Immunoreactivity for P-170 glycoprotein in malignant and in non-neoplastic mesothelium of the pleura arising the murine monoclonal antibody JSB-1. J Pathol 1992;167:5–8.
13 Segers K, Kumar-Singh S, Weyler J, *et al*. Immunoreactivity for bcl-2 protein in malignant mesothelioma and non-neoplastic mesothelium. Virchows Arch 1994;242:631–634.
14 Olson AL, Pessin JE. Structure, function, and regulation of the mammalian facilitative glucose transporter gene family. Annu Rev Nutr 1996;16:235–256.
15 Younes M, Lechago LV, Somoano JR, *et al*. Wide expression of the human erythrocyte glucose transporter Glut1 in human cancers. Cancer Res 1996;56: 1164–1167.
16 Godoy A, Ulloa V, Rodriguez F, *et al*. Differential subcellular distribution of glucose transporters GLUT1-6 and GLUT9 in human cancer: ultrastructural localization of GLUT1 and GLUT5 in breast tumor tissues. J Cell Physiol 2006;207:614–627.
17 Brown RS, Wahl RL. Overexpression of Glut-1 glucose transporter in human breast cancer. An immunohistochemical study. Cancer 1993;72:2979–2985.
18 Mellanen P, Minn H, Grenman R, *et al*. Expression of glucose transporters in head-and-neck tumors. Int J Cancer 1994;56:622–629.
19 Nagase Y, Takata K, Moriyama N, *et al*. Immunohistochemical localization of glucose transporters in human renal cell carcinoma. J Urol 1995;153:798–801.
20 Younes M, Brown RW, Stephenson M, *et al*. Overexpression of Glut1 and Glut3 in stage I nonsmall cell lung carcinoma is associated with poor survival. Cancer 1997;80:1046–1051.
21 Ito T, Noguchi Y, Satoh S, *et al*. Expression of facilitative glucose transporter isoforms in lung carcinomas: its relation to histologic type, differentiation grade, and tumor stage. Mod Pathol 1998;11:437–443.
22 Brown RS, Leung JY, Kison PV, *et al*. Glucose transporters and FDG uptake in untreated primary human non-small cell lung cancer. J Nucl Med 1999;40:556–565.
23 Chang S, Lee S, Lee C, *et al*. Expression of the human erythrocyte glucose transporter in transitional cell carcinoma of the bladder. Urology 2000;55:448–452.
24 Mamede M, Higashi T, Kitaichi M, *et al*. [18F]FDG uptake and PCNA, Glut-1, and Hexokinase-II expressions in cancers and inflammatory lesions of the lung. Neoplasia 2005;7:369–379.

25 Weiner MF, Miranda RN, Bardales RH, *et al*. Diagnostic value of GLUT-1 immunoreactivity to distinguish benign from malignant cystic squamous lesions of the head and neck in fine-needle aspiration biopsy material. Diagn Cytopathol 2004;31:294–299.
26 Chandan VS, Faquin WC, Wilbur DC, *et al*. The utility of GLUT-1 immunolocalization in cell blocks: an adjunct to the fine needle aspiration diagnosis of cystic squamous lesions of the head and neck. Cancer 2006;108:124–128.
27 Burstein DE, Reder I, Weiser K, *et al*. GLUT1 glucose transporter: a highly sensitive marker of malignancy in body cavity effusions. Mod Pathol 1998;11:392–396.
28 Zimmerman RL, Goonewardene S, Fogt F. Glucose transporter Glut-1 is of limited value for detecting breast carcinoma in serous effusions. Mod Pathol 2001;14:748–751.
29 Afify A, Zhou H, Howell L, *et al*. Diagnostic utility of Glut-1 expression in the cytologic evaluation of serous fluids. Acta Cytol 2005;49:621–626.
30 Churg A, Roggli V, Galateau-Salle F, *et al*. Mesothelioma. In: Travis WD, Brambilla E, Muller-Hermelink HK, Harris CC (eds). Pathology and Genetics: Tumors of the Lung, Pleura, Thymus and Heart. IARC: Lyon, France, 2004, pp 128–136.
31 Ordonez NG. Immunohistochemical diagnosis of epithelioid mesothelioma: an update. Arch Pathol Lab Med 2005;129:1407–1414.
32 Merrall NW, Plevin R, Gould GW. Growth factors, mitogens, oncogenes and the regulation of glucose transport. Cell Signal 1993;5:667–675.
33 Mueckler M. Facilitative glucose transporters. Eur J Biochem 1994;219:713–725.
34 Clavo AC, Brown RS, Wahl RL. Fluorodeoxyglucose uptake in human cancer cell lines is increased by hypoxia. J Nucl Med 1995;36:1625–1632.
35 Newsholme EA, Board M. Application of metabolic-control logic to fuel utilization and its significance in tumor cells. Adv Enzyme Regul 1991;31:225–246.
36 Carretta A, Landoni C, Melloni G, *et al*. 18-FDG positron emission tomography in the evaluation of malignant pleural diseases–a pilot study. Eur J Cardiothorac Surg 2000;17:377–383.

Proteomic Signature Corresponding to the Response to Gefitinib (Iressa, ZD1839), an Epidermal Growth Factor Receptor Tyrosine Kinase Inhibitor in Lung Adenocarcinoma

Tetsuya Okano,[1,6] Tadashi Kondo,[1] Kiyonaga Fujii,[2] Toshihide Nishimura,[2] Toshimi Takano,[4] Yuichiro Ohe,[4] Koji Tsuta,[5] Yoshihiro Matsuno,[5] Akihiko Gemma,[6] Harbumi Kato,[2,3] Shoji Kudoh,[6] and Setsuo Hirohashi[1]

Abstract **Purpose:** We aimed to identify candidate proteins for tumor markers to predict the response to gefitinib treatment.

Experimental Design: We did two-dimensional difference gel electrophoresis to create the protein expression profile of lung adenocarcinoma tissues from patients who showed a different response to gefitinib treatment. We used a support vector machine algorithm to select the proteins that best distinguished 31 responders from 16 nonresponders. The prediction performance of the selected spots was validated by an external sample set, including six responders and eight nonresponders. The results were validated using specific antibodies.

Results: We selected nine proteins that distinguish responders from nonresponders. The predictive performance of the nine proteins was validated examining an additional six responders and eight nonresponders, resulting in positive and negative predictive values of 100% (six of six) and 87.5% (seven of eight), respectively. The differential expression of one of the nine proteins, heart-type fatty acid–binding protein, was successfully validated by ELISA. We also identified 12 proteins as a signature to distinguish tumors based on their *epidermal growth factor receptor* gene mutation status.

Conclusions: Study of these proteins may contribute to the development of personalized therapy for lung cancer patients.

Non-small cell lung carcinoma (NSCLC) accounts for ~85% of lung cancer cases (1). Biomarker(s) that predict the response to gefitinib (Iressa; AstraZeneca, Macclesfield, United Kingdom), an epidermal growth factor receptor (EGFR) tyrosine kinase inhibitor, may help to improve the choice of therapeutic strategy in patients with NSCLC. Gefitinib improves NSCLC-related symptoms and quality of life in some patients with advanced NSCLC who do not respond to platinum-based chemotherapy. However, the response rate for gefitinib remains <20% in patients with NSCLC (2–4), and treatment with gefitinib is associated with serious adverse effects, such as severe acute interstitial pneumonia in 5.4% of the patients who received the treatment (5, 6). Thus, it is imperative to select appropriate patients for treatment with gefitinib and exclude patients in whom gefitinib is unlikely to exhibit any clinical benefit. Women, patients who have never smoked, patients with adenocarcinoma, and East Asians are major subgroups of responders (3, 4, 6–8). Recently, gain-of-function somatic mutation in the tyrosine kinase domain of the EGFR has been correlated with the response to gefitinib (9, 10). However, other studies have revealed that correction of the phenotype arising from EGFR mutation may not account for all of the clinical benefits of gefitinib (11, 12), and both preclinical and clinical studies have reported that the efficacy of gefitinib is independent of EGFR expression level (11, 13–15). Although molecular features of the *EGFR* gene, including mutation and high copy number, (16, 17) are associated with response to gefitinib, other molecular markers in the tumor, such as HER2 overexpression (18), Akt phosphorylation (19), and other EGFR downstream molecules (20), also correlate with response. These observations suggest a role for unknown, but important, factors in gefitinib sensitivity. Identification and elucidation of such factors will improve existing therapeutic protocols and contribute to further understanding of the mechanisms of gefitinib sensitivity.

Authors' Affiliations: [1]Proteome Bioinformatics Project, National Cancer Center Research Institute; [2]Clinical Proteome Center and [3]Department of Surgery, Tokyo Medical University; [4]Department of Internal Medicine and [5]Clinical Laboratory Division, National Cancer Center Hospital; and [6]The Fourth Internal Department of Medicine, Nippon Medical School, Tokyo, Japan

Received 7/7/06; revised 11/17/06; accepted 11/29/06.

Grant support: 'Third-Term Comprehensive Control Research for Cancer' conducted by the Ministry of Health, Labor, and Welfare and by the Program for Promotion of Fundamental Studies in Health Sciences in the National Institute of Biomedical Innovation of Japan. Tetsuya Okano is the recipient of a Research Resident Fellowship from the Foundation for Promotion of Cancer Research (Japan).

The costs of publication of this article were defrayed in part by the payment of page charges. This article must therefore be hereby marked *advertisement* in accordance with 18 U.S.C. Section 1734 solely to indicate this fact.

Note: Supplementary data for this article are available at Clinical Cancer Research Online (http://clincancerres.aacrjournals.org/).

Current address for K. Fujii: Proteome Bioinformatics Project, National Cancer Center Research Institute, Tokyo, Japan.

Requests for reprints: Tadashi Kondo, Proteome Bioinformatics Project, National Cancer Center Research Institute, 5-1-1 Tsukiji, Chuo-ku, Tokyo 104-0045, Japan. Phone: 81-3-3542-2511, ext. 3004; Fax: 81-3-3457-5298; E-mail: takondo@gan2.res.ncc.go.jp.

doi:10.1158/1078-0432.CCR-06-1654

To identify the gene products correlated with the efficacy of gefitinib, genome-wide screening was done recently for NSCLC. A global mRNA expression study using DNA microarrays and biopsy samples identified 51 genes associated with the sensitivity to gefitinib and established a numerical scoring system to predict the response (21). This expression study also led to the establishment of ELISA assays for the identified gene products in serum. Preclinical studies involving mRNA profiling of NSCLC xenografts resulted in the identification of a set of genes that were differentially expressed between tumors that were sensitive and insensitive to gefitinib treatment (22, 23). These studies will lead to the identification of novel biomarkers to predict the response to gefitinib treatment. However, mRNA expression does not necessarily correlate with protein level, and posttranslational modifications, such as phosphorylation, cannot be predicted from the amount of RNA or from the DNA sequence (24). With this background, comprehensive expression studies at the protein level, an approach called proteomics, have been conducted in patients with lung cancer to develop biomarkers that predict clinical outcomes (25). However, no global protein expression study has yet been done on the mechanism of response to gefitinib.

To identify the proteomic signature for sensitivity to gefitinib and to use that signature as a tumor marker to predict the response to gefitinib, we analyzed global protein expression levels in lung adenocarcinoma tissues for whom we have detailed information on *EGFR* gene status. The surgical specimens were obtained at the time of surgery from patients who subsequently had recurrence and received gefitinib monotherapy. We then used two-dimensional difference gel electrophoresis (2D-DIGE) covering ~2,000 proteins to identify a set of proteins of which expression was associated with sensitivity to gefitinib and with EGFR mutation. The predictive performance of the protein set was validated with an independent data set and compared with that of EGFR mutation.

Materials and Methods

Patients and tissue samples. We examined tumor tissues from patients who relapsed after surgery and received gefitinib monotherapy. Two hundred seventy-nine patients who received gefitinib at the National Cancer Center Hospital from July 2002 to December 2004 were evaluated for inclusion in this study. Ninety-two patients relapsed after surgical resection of primary NSCLC and started to receive monotherapy with gefitinib 250 mg/d for 14 days ($n = 92$). We used tumor tissues obtained at the time of surgery and stored in vapor nitrogen. Fifteen patients were excluded from our study for the following reasons: frozen tissues were not available ($n = 10$) and tumor histology showed squamous cell carcinoma ($n = 4$) or pleomorphic carcinoma ($n = 1$). The histologic features of the tissues were reviewed by two board-certified pathologists (Y.M and K.T.) and diagnosis was based on the latest WHO classification of lung adenocarcinoma (8, 26–28). The tumor responses were classified into complete response (CR), partial response (PR), and progressive disease (PD) using standard bidimensional measurements (29). In this study, patients without a marked reduction of tumor size were subdivided into minor response (MR) and stable disease (SD) groups. MR was defined as a 25% decrease in the sum of the products of perpendicular diameters of all measurable lesions at any point during gefitinib treatment. SD was defined as a <25% decrease in tumor size after treatment. The clinical information is summarized in Table 1, and further information, including EGFR mutation status, is summarized in Supplementary Table S1. Consent was obtained from all patients and the protocol was approved by the institutional review board of the National Cancer Center.

To identify the proteins associated with response to gefitinib, we compared the protein expression profiles of responders (CR and PR) and nonresponders (PD). Of 77 samples available, the effects of gefitinib treatment were not examined for six cases because the treatment was not completed. These six samples were excluded from this study. We constructed two sample sets in the following way (Table 2): a training sample set comprising 31 responders (2 CRs + 29 PRs) and 16 nonresponders (16 PDs) and a test set comprising six responders (6 PRs) and 8 nonresponders (8 PDs) from whom samples were obtained between June and December 2004 (Table 2). As no significant differences were observed between CRs and PRs (Supplementary Fig. S1A), we grouped CRs and PRs together in the responder group.

Protein extraction and protein expression profiling. The frozen tumor tissues were crushed to frozen powder with a Multi-Beads Shocker (Yasui-kikai, Osaka, Japan) under cooling with liquid nitrogen. The frozen powder was then treated with urea lysis buffer (7 mol/L urea, 2 mol/L thiourea, 3% CHAPS, 1% Triton X-100) for 30 min on ice. After centrifugation at 15,000 rpm for 30 min, the supernatant was recovered as cellular protein for the protein expression study.

Protein samples were labeled with CyDye DIGE Fluor saturation dye (GE Healthcare Amersham Biosciences, Uppsala, Sweden) according to

Table 1. Patient characteristics

	No. patients	%
Gender		
Female	33	43
Male	44	57
Age (y)		
Median (range)	62.2 (32-80)	—
Histologic type		
Adenocarcinoma		100
Papillary/acinar/bronchioloalveolar/solid	30/16/9/6	49/26/15/10
Smoking history*		
Never smokers	37	48
Former smokers	12	16
Current smokers	28	36
ECOG performance status†		
0/1/2/3	24/39/9/5	31/51/12/6
Prior chemotherapy		
Yes	30	39
No	47	61
Response to gefinitib		
CR/PR/MR/SD/PD/NE	2/35/2/8/24/6	3/45/3/10/31/8
EGFR gene status		
Mutation L858R	18	23.4
DEL‡	18	23.4
G719§	2	2.6
Wild-type	35	45.4
Unknown	4	5.2

Abbbreviation: NE, not evaluated.
*Never-smokers: those who had never had a smoking habit; former smokers: those who had stopped smoking at least 1 yr before diagnosis; and current smokers: active smokers at diagnosis of NSCLC or those who had stopped smoking less than 1 yr before diagnosis.
†ECOG performance status was monitored according to the previous report (44).
‡Deletional mutations in exon 19.
§G719S and G719C.

Table 2. Training and test sets to develop the classifier for the response to gefitinib

	Training set			Test set		
	Responders, $n = 31$ (%)	Nonresponders, $n = 16$ (%)	P	Responders, $n = 6$ (%)	Nonresponders, $n = 8$ (%)	P
Age						
Mean ± SD	64.0 ± 8.9	60.5 ± 12.0	0.330	57.5 ± 12.8	62.8 ± 6.1	0.386
Gender						
Male	17 (55)	9 (56)	0.927	3 (50)	5 (62.5)	0.640
Female	14 (45)	7 (44)		3 (50)	3 (37.5)	
Smoking history						
Never smokers	17 (55)	9 (56)	0.286	4 (67)	4 (50)	0.054
Former smokers	7 (22.5)	1 (6)		2 (33)	0 (0)	
Current smokers	7 (22.5)	6 (38)		0 (0)	4 (50)	
EGFR gene status						
Mutation	27 (87)	1 (6)	<0.001	4 (66)	0 (0)	0.006
Wild type	3 (10)	13 (81)		1 (17)	8 (100)	
Unknown	1 (3)	2 (13)		1 (17)	0 (0)	
Prior chemotherapy						
(+)	12 (39)	5 (31)	0.614	6 (100)	0 (22)	<0.001
(−)	19 (61)	11 (69)		0 (0)	8 (100)	
Performance status						
0	11 (35.5)	6 (37.5)	0.945	2 (33)	1 (12.5)	0.347
1	11 (35.5)	10 (62.5)		4 (67)	7 (87.5)	
2	6 (19)	0 (0)		0 (0)	0 (0)	
3	3 (10)	0 (0)		0 (0)	0 (0)	

our previous report (30). We prepared an internal control consisting of a mixture of small portions of all protein samples obtained before May 2004 (31). The internal control sample and the individual experimental samples were labeled with Cy3 and Cy5 CyDye DIGE Fluor saturation dyes, respectively. Five micrograms of Cy3- or Cy5-labeled protein were mixed and coseparated by two-dimensional PAGE. The first-dimension separation was achieved on an Immobiline pH gradient gel (isoelectric point range, 4-7; 24 cm length) with a Multiphor II (GE Healthcare Amersham Biosciences). The second-dimension separation was done with an EttanDalt II (GE Healthcare Amersham Biosciences) with a 9% to 15% gradient polyacrylamide gel. After electrophoresis, the gels were scanned at appropriate wavelengths for Cy3 and Cy5 (Supplementary Fig. S2A). The ratio between Cy5 and Cy3 intensity was calculated for all protein spots in identical gels by the use of DeCyder software (GE Healthcare Amersham Biosciences; ref. 31). The standardized spot intensities were then logarithmically transformed and subjected to a data-mining package (Impressionist; GeneData, Basel, Switzerland). We ran triplicate gels for each sample and calculated the averaged standardized spot intensity.

To assess the reproducibility of the proteomic data with the internal control in our analyses, we generated triplicate protein profiles from identical samples (case 9; Supplementary Table S1) and compared the standardized intensity of the paired spots (Supplementary Fig. S2B). Scattergrams with 1,980, 1,646, and 1,873 spots showed that the intensities of 1,916 (93.7%), 1,599 (94.7%), and 1,770 (94.5%) spots, respectively, were scattered within a 2-fold difference, and the correlation values were also high (r values > 0.93; Supplementary Fig. S2B).

Data analysis. A bioinformatic approach based on a support vector machine (SVM) algorithm and a leave-one-out cross-validation was used to identify proteins of which expression was associated with tumor characteristics, including therapeutic response to gefitinib and the presence of EGFR mutation (32).

Protein identification. Proteins corresponding to the protein spots of interest were identified by mass spectrometry (30). The proteins were recovered in a gel plug by using an automated spot collector (SpotPicker; GE Healthcare Amersham Biosciences) and digested with sequence grade trypsin (Promega, Madison, WI; ref. 30). Trypsin digests were applied to liquid chromatography coupled with tandem mass spectrometry (LTQ, Thermo, Waltham, MA). A database search against Swiss-Prot was done with Mascot software. Patients with a Mascot score of 35 or more were used for protein identification. When multiple proteins were identified in a single spot, the proteins with the highest number of peptides were considered as those corresponding to the spot.

Mutations in the EGFR gene. EGFR mutations in the samples obtained between July 2002 and May 2004 were examined as described in our previous report (8). Analysis of samples obtained between June 2004 and December 2004 was done by high-resolution melting analysis with a LightCycler HR-1 system (Idaho Technology Inc., Salt Lake City, UT).

ELISA. The expression level of heart-type fatty acid–binding protein (H-FABP) in protein samples from 55 lung adenocarcinoma patients (2 CRs, 28 PRs, 6 SDs, 1 MR, and 18 PDs) was measured in a clinical laboratory (SRL, Tokyo, Japan) with a commercially available ELISA kit (MARKIT-M H-FABP, Dainippon Pharmaceutical, Tokyo, Japan) according to the manufacturer's instructions (Supplementary Table S1). All these 55 samples were included in a 2D-DIGE analysis set in this study.

Results

Proteomic signature for the response to gefitinib. We first selected 1,685 protein spots that appeared in at least 80% of the images of Cy3-labeled internal control. We further selected 87 protein spots that showed different intensities between responder and nonresponder groups ($P < 0.05$, Wilcoxon test). Although potentially resulting in a loss of information, this trimming process decreased the possibility that the classifier would be significantly influenced by irrelevant expression data. We selected protein sets for which expression was associated with response to gefitinib by using a SVM algorithm. Accuracy, plotted as a function of spot number, was constant until the number of spots decreased to less than nine, showing that accurate classification did not require all protein spots (Fig. 1A). The location on the two-dimensional map is shown for the selected nine spots (Fig. 1B; Supplementary Fig. S3).

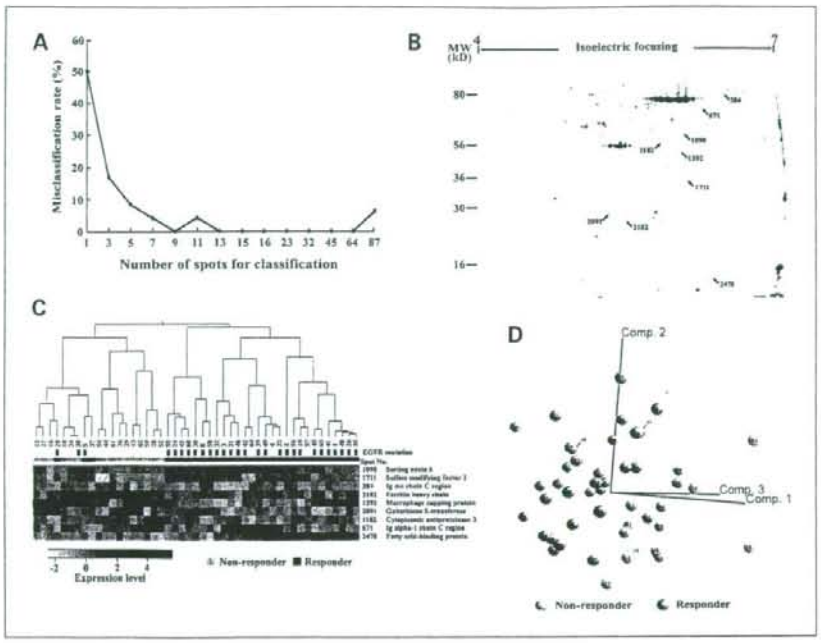

Fig. 1. Data-mining procedure to develop the prediction model for the response to gefitinib. *A*, a spot ranking method selected a few protein spots by which the cumulative error rate of a leave-one-out cross-validation became minimal. The spot ranking method indicated that the error rate was minimal when the prediction model was constructed by a particular nine protein spots. *B*, localization of the selected nine protein spots on the two-dimensional map. An enlarged two-dimensional image is shown in Supplementary Fig. S2. *C*, hierarchical clustering analysis of the samples in the learning set using the selected nine protein spots. Black bars, the presence of EGFR mutations within exons 18 to 21. *D*, principal component analysis of the samples in the learning set using the selected nine protein spots. Comp.1, 2, and 3, the first component 1, 2, and 3, respectively.

Mass spectrometry revealed that these nine spots corresponded to nine gene products (Table 3). Overall similarity of the selected spots is shown in Supplementary Fig. S1B and C. As the responder group in the training set consisted mainly of PRs, the obtained proteomic signature would presumably be more reflective of PR than CR.

The classification performance of the selected nine protein spots was validated by unsupervised classification. Hierarchical clustering showed that all tumor samples in the training set, except for cases 5, 20, and 37, were grouped according to their sensitivity to gefitinib based on the expression pattern of the nine proteins (Fig. 1C). In principal component analysis, all 47 samples seemed to be separated into two groups, although the border between these groups was not clear (Fig. 1D). Although hierarchical clustering and principal component analysis are crude methods of validation of classification, the results obtained using them were consistent.

To validate the predictive performance of the nine protein spots, we investigated a newly enrolled test sample set that was completely independent of the learning set. Based on the expression level of the nine protein spots, the distance of each sample from the hyperplane created by the SVM algorithm, defined as the SVM value, was calculated. The samples with a positive SVM value were grouped as responders and the samples with a negative SVM value were grouped as nonresponders. As a consequence, all training set samples were correctly classified in accordance with their clinical response to gefitinib (Fig. 2). All responders (six PRs) and seven of eight nonresponders (eight PDs) in the test set were also correctly classified. The expression pattern of the nine protein spots in the nonresponder patient (case 75) was more similar to that of the responder group, for unknown reasons. We also validated the results using the samples from patients who showed MR and SD. We found that the two patients showing MR were categorized as responders and that among the eight patients showing three SDs were classified into the responder group and five SDs into the nonresponder group. We did a leave-one-out cross validation for all 47 samples in the training set and the test set using nine protein spots with 1,000 times random permutation. All but two cases, cases 37 and 75, were correctly classified according to their status of response to the treatment. The overall misclassification error rate was 3.3%. Consequently, the model predicted the response to gefitinib in 13 of the 14 (92.8%) newly enrolled samples from the responders and nonresponders and may be useful for disease monitoring.

Proteomic signature for EGFR gene mutation. We studied the spots on the prediction for EGFR mutation. We set a training sample set, including 58 samples (34 mutation-positive samples and 24 mutation-negative samples; Supplementary Table S2). We found that the 12 protein spots showed the high correlation with the EGFR mutation (Supplementary Data; Supplementary Figs. S4-6). The classification and prediction performance of the selected 12 protein spots was successfully validated using the external validation sample set, including four mutation-positive samples and 11 mutation-negative samples (Supplementary Fig. S7). Only one protein, sulfate modifying factor 2, was shared between the signatures for the response and for the mutation (Table 3; Supplementary Table S3).

Expression of H-FABP measured by ELISA. We validated the differential expression of the identified proteins by the use of a widely available clinical assay. The expression level of H-FABP in the same tumor samples as those used in 2D-DIGE was measured with a commercially available ELISA kit intended for serum assays (Fig. 3). H-FABP expression measured by ELISA was highly correlated with that measured by 2D-DIGE (Pearson correlation, 0.76295; $P < 0.0001$). The ELISA study also showed